ISSN 2096-7071 (Print)
ISSN 2096-3101 (Online)
CN 10-1629/R1

CHINA CDC WEEKLY

Vol. 6 No. 27 Jul. 5, 2024

CCDC weekly

中国疾病预防控制中心周报

INFECTIOUS DISEASE ISSUE

Preplanned Studies

Trends in Incidence of HIV and Syphilis Among Men Who Have Sex with Men — Tianjin Municipality, China, 2013–2022 651

Effectiveness of Frequent Viral Load Testing Plus Additional Interventions to Prevent HIV Transmission in Heterosexual, Serodiscordant Couples — Yunnan Province, China, 2019–2021 658

Vital Surveillances

The Epidemiological Characteristics and Spatiotemporal Clustering of Measles — China, 2005–2022 665

Methods and Applications

A New Integrated Interpolation Method for High Missing Unstable Disease Surveillance Data — 12 Urban Agglomerations, China, 2009–2020 670

Outbreak Reports

A Case of Brucellosis Concomitant with Severe Fever with Thrombocytopenia Syndrome — Weifang City, Shandong Province, China, 2023 677

ISSN 2096-7071

China CDC Weekly

Editorial Board

Editor-in-Chief Hongbing Shen
Founding Editor George F. Gao
Deputy Editor-in-Chief Liming Li Gabriel M Leung Zijian Feng
Executive Editor Chihong Zhao
Members of the Editorial Board

Rui Chen	Wen Chen	Xi Chen (USA)	Zhuo Chen (USA)
Gangqiang Ding	Xiaoping Dong	Pei Gao	Mengjie Han
Yuantao Hao	Na He	Yuping He	Guoqing Hu
Zhibin Hu	Yueqin Huang	Na Jia	Weihua Jia
Zhongwei Jia	Guangfu Jin	Xi Jin	Biao Kan
Haidong Kan	Ni Li	Qun Li	Ying Li
Zhenjun Li	Min Liu	Qiyong Liu	Xiangfeng Lu
Jun Lyu	Huilai Ma	Jiaqi Ma	Chen Mao
Xiaoping Miao	Ron Moolenaar (USA)	Daxin Ni	An Pan
Lance Rodewald (USA)	William W. Schluter (USA)	Yiming Shao	Xiaoming Shi
Yuelong Shu	RJ Simonds (USA)	Xuemei Su	Chengye Sun
Quanfu Sun	Xin Sun	Feng Tan	Jinling Tang
Huaqing Wang	Hui Wang	Linhong Wang	Tong Wang
Guizhen Wu	Jing Wu	Xifeng Wu (USA)	Yongning Wu
Min Xia	Ningshao Xia	Yankai Xia	Lin Xiao
Wenbo Xu	Hongyan Yao	Zundong Yin	Dianke Yu
Hongjie Yu	Shicheng Yu	Ben Zhang	Jun Zhang
Liubo Zhang	Wenhua Zhao	Yanlin Zhao	Xiaoying Zheng
Maigeng Zhou	Xiaonong Zhou	Guihua Zhuang	

Advisory Board

Director of the Advisory Board Jiang Lu
Vice-Director of the Advisory Board Yu Wang Jianjun Liu Jun Yan
Members of the Advisory Board

Chen Fu	Gauden Galea (Malta)	Dongfeng Gu	Qing Gu
Yan Guo	Ailan Li	Jiafa Liu	Peilong Liu
Yuanli Liu	Kai Lu	Roberta Ness (USA)	Guang Ning
Minghui Ren	Chen Wang	Hua Wang	Kean Wang
Xiaoqi Wang	Zijun Wang	Fan Wu	Xianping Wu
Jingjing Xi	Jianguo Xu	Gonghuan Yang	Tilahun Yilma (USA)
Guang Zeng	Xiaopeng Zeng	Yonghui Zhang	Bin Zou

Editorial Office

Directing Editor Chihong Zhao
Managing Editors Yu Chen
Senior Scientific Editors Daxin Ni Ning Wang Wenwu Yin Shicheng Yu Jianzhong Zhang Qian Zhu
Scientific Editors

Weihong Chen	Tao Jiang	Xudong Li	Nankun Liu	Liwei Shi	Liuying Tang
Meng Wang	Zhihui Wang	Qi Yang	Qing Yue	Lijie Zhang	Ying Zhang

Cover Photo: Farm staff collected blood samples from sheep for brucellosis test, Shandong Province, 2023. Credited from this week's author Hai Jiang, National Institute for Communicable Disease Control and Prevention, China CDC.

Preplanned Studies

Trends in Incidence of HIV and Syphilis Among Men Who Have Sex with Men — Tianjin Municipality, China, 2013–2022

Yan Guo[1,&]; Fangfang Chen[2,&]; Hui Gong[1]; Ziming Wu[1]; Xinying Zhang[3]; Tielin Ning[1]; Zhongquan Liu[1]; Jianyun Bai[1]; Long Li[1]; Jie Yang[4]; Fangning Zhao[1]; Jinyu Hou[1]; Maohe Yu[1,5,#]; Houlin Tang[2,#]

Summary

What is already known about this topic?

Given the common modes of transmission, outbreaks of both human immunodeficiency virus (HIV) and syphilis are primarily observed in men who have sex with men (MSM). However, minimal research has been conducted to concurrently evaluate the rates and trends of HIV and syphilis incidence within this community in China.

What is added by this report?

This manuscript presents the incidence rates and associated factors of HIV and syphilis in MSM in Tianjin based on data derived from a decade-long cohort study. Intriguingly, it depicts a decreasing trend in HIV incidence juxtaposed with an increasing incidence of syphilis among this population in Tianjin.

What are the implications for public health practice?

The interconnected risk factors for HIV and syphilis pose significant hindrances to disease control. Our study underscores the urgent need for improved intervention strategies specifically aimed at MSM to mitigate the propagation of both infections.

Human immunodeficiency virus (HIV) continues to pose a significant public health threat, particularly among men who have sex with men (MSM). In 2022 (*1*), the global tally of new HIV infections approximated at 1.3 million, with HIV incidence among MSM reportedly nearly five per 100 person-years (PYs), 27 to 150 times higher than that in the general adult male population (*2*). Alarmingly, China has observed an uptick in HIV instances among MSM (*3*). Concurrently, syphilis resurfaced as a major public health concern, predominantly affecting the MSM community (*4*). Despite this pronounced escalation, insight into the extent and trajectory of HIV and syphilis incidence among MSM in China remains inadequate. In Tianjin Municipality, for instance, case reports suggest MSM constitute approximately 80% of HIV/acquired immune deficiency syndrome (HIV/AIDS) instances (*5*), mirrored by a high prevalence of syphilis within the demographic (*6*). Comprehending the dynamics behind these incidence rates is critical in monitoring and appraising public health approaches. To that end, a cohort study involving 2,110 participants for HIV and 1,927 for syphilis was conducted among the MSM population in Tianjin from 2013 to 2022. The study revealed a declining trend in HIV incidence of an average rate of 2.3 per 100 PYs over the study period, contrasted by a rising trend in syphilis incidence of an average rate of 4.8 per 100 PYs. These findings, via multivariate analysis, pinpointed several factors linked to HIV and syphilis incidence, emphasizing the imperative to amplify intervention initiatives for MSM to mitigate HIV and syphilis transmission.

From April 2013 to March 2022, an open cohort study was conducted focusing on MSM based in Tianjin. Inclusion criteria for participants were: biological male , being at least 16 years old, engaging in oral or anal intercourse with males in the past year, voluntary completion of questionnaires and registration with fingerprints, submission to blood sampling for HIV and syphilis testing, a negative or unknown HIV/syphilis status at the initial survey, and having at least two HIV/syphilis test records during the study period. Exclusion criteria included inability to participate independently in the survey, and pre-existing HIV/syphilis infection prior to the initial survey. Between April 2013 and March 2022, MSM were recruited via online and offline methods through community-based organizations, creating an open cohort. All participants were required to provide baseline data relating to demographics, behavioral factors, and HIV/syphilis status, with information collected through structured questionnaires administered by trained interviewers. Participants were then followed up every six months for serological testing for HIV and syphilis. HIV testing used an enzyme-linked immunosorbent assay (ELISA; Wantai

Biotech Inc., China and Lizhu Biotech Inc., Beijing, China) and any positive results were confirmed by western blotting (HIV Blot 2.2; MP Diagnostics, Singapore). Syphilis testing also used an ELISA test (Yingke-xinchuang Biotech Inc., China), but positive results were confirmed using a toluidine red unheated serum test (TRUST; Wantai Biotech Inc., China). Syphilis was diagnosed only when both ELISA and TRUST tests were positive (*7*). After excluding participants who tested HIV positive at the baseline (n=123), or lacked follow-up records (n=557), 2,110 MSM were included in the final data analysis to estimate HIV incidence (Figure 1). Of those 2,110 participants, 183 tested positive for syphilis at baseline; hence, the remaining 1,927 MSM who tested syphilis-negative were included in the final data analysis for syphilis incidence estimation. Follow-up PYs were calculated from the date of the baseline survey to the last HIV/syphilis test, date of death, loss to follow-up, or March 31, 2022 — whichever occurred first. Incidence rates for HIV and syphilis were then calculated based on seroconversions and observed PYs.

Categorical variables were delineated in terms of frequencies and percentages, whereas continuous variables were displayed as "Median (lower quartile, upper quartile)". To estimate the hazard ratios (*HR*) and 95% confidence intervals (*CI*) for HIV and syphilis incidences, Cox proportional hazards (PH) models were utilized. All statistical analyses, including two-sided tests with a significance level of P<0.05, were carried out using SPSS software (version 24.0; Armonk, NY: IBM Corp.). The study received ethical approval from the Ethics Committee of the Center for STD and AIDS Prevention and Control of the Chinese Center for Disease Control and Prevention (X130419285).

The median age for the 2,110 participating MSM was determined to be 27.5 years, with an interquartile range (IQR) of 24.0 to 34.0 years. Demographic analysis revealed that 60.5% of the participants were local residents, 74.7% were single, and 88.9% had acquired at least a high school level education. In terms of sexual orientation, 84.5% identified themselves as homosexual.

During the observation period, there were 151 reported HIV seroconversions within 6,486.0 PYs, establishing an HIV incidence rate of 2.3 per 100 PYs (95% *CI*: 2.0, 2.7). To minimize the effects of random errors and facilitate a comprehensive assessment of incidence trends, the 2-year incidence rate was utilized.

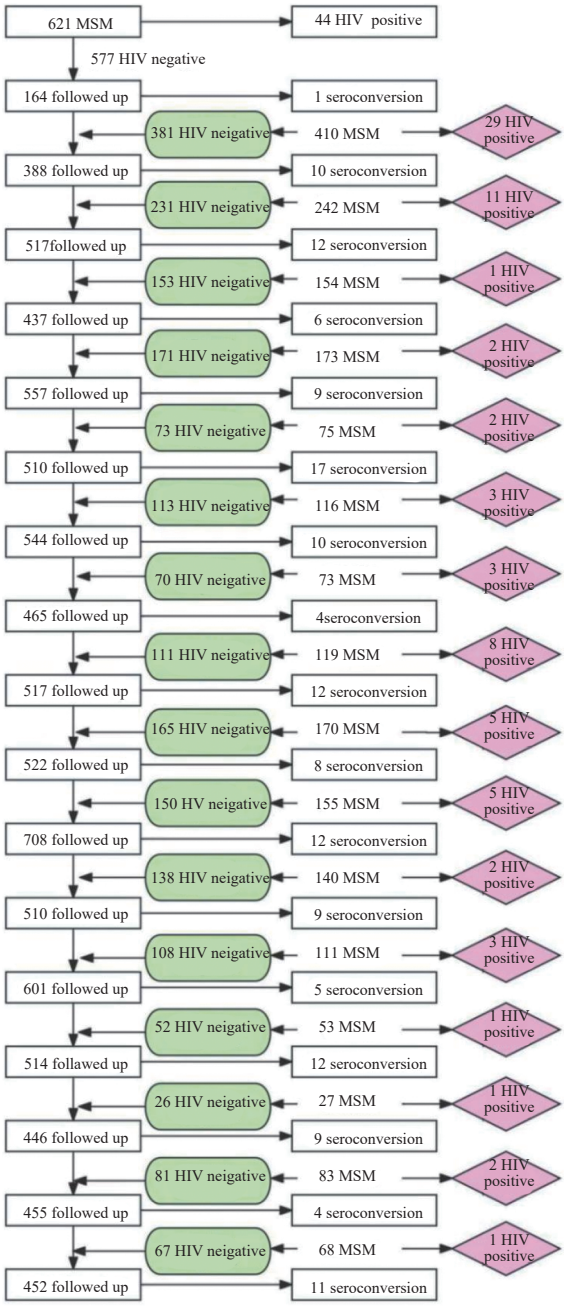

FIGURE 1. Process of the retrospective cohort study among MSM in Tianjin Municipality, China.
Abbreviation: HIV=human immunodeficiency virus; MSM=men who have sex with men.

HIV incidence rates varied over time, reaching a peak of 5.2 (95% *CI*: 3.2, 7.2) in 2013–2014, before dropping to 4.2 (95% *CI*: 3.0, 5.4) in 2015–2016, 2.4 (95% *CI*: 1.7, 3.1) in 2017–2018, 2.2 (95% *CI*: 1.5, 2.9) in 2019–2020, and 1.9 (95% *CI*: 0.9, 2.9) per 100 PYs in 2021–2022 (Figure 2). The PH assumption for the Cox models was validated by examining the interaction terms between the variables

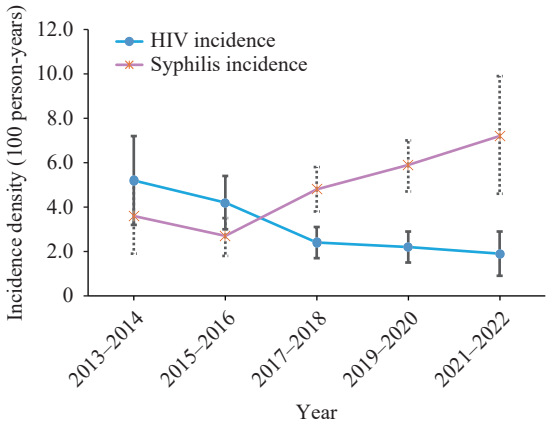

FIGURE 2. Trends in the incidence of HIV and syphilis among MSM in Tianjin Municipality, China, from 2013 to 2022.
Abbreviation: HIV=human immunodeficiency virus; MSM=men who have sex with men.

included in the model and the log of follow-up time, with no violations observed. Therefore, Cox PH models were employed to estimate the associations between various factors and HIV/syphilis incidence. The multivariate analysis demonstrated that MSM identifying as heterosexual or bisexual had a lower risk of HIV incidence than those identifying as homosexual [adjusted hazard ratio (aHR)=0.597, 95% *CI*: 0.358, 0.996]. MSM who engaged in unprotected anal sex during the previous six months had a 43.6% increased risk of HIV incidence (aHR=1.436, 95% *CI*: 1.014, 2.033) compared to those who did not. Furthermore, MSM who experienced their first homosexual intercourse at 20 years old or later were found to be at a 46.7% higher risk of HIV incidence (aHR=1.467, 95% *CI*: 1.023, 2.104) compared to those who first engaged in homosexual intercourse at a younger age. The risk of HIV incidence was also higher among MSM who used psychoactive substances within the last six months (aHR=1.584, 95% *CI*: 1.137, 2.207). Conversely, regular follow-up visits (more than thrice) seemed to serve as a protective factor against HIV incidence (aHR=0.216, 95% *CI*: 0.152, 0.308) in comparison to those with two or fewer follow-ups during the study period. Syphilis infection proved to be a significant risk factor for HIV incidence among MSM (aHR=1.795, 95% *CI*: 1.131, 2.849) (Table 1).

In the study, 1,927 participants contributed to syphilis incidence evaluation by providing 5,469.3 PYs of follow-up data. Throughout this period, 260 new syphilis cases were identified, which yielded an incidence rate of 4.8 per 100 PYs (95% *CI*: 4.2, 5.3). A pattern of escalating syphilis incidence rates was witnessed over the years, increasing from 3.6 (95% *CI*: 1.9, 5.3) in 2013–2014, 2.7 (95% *CI*: 1.9, 3.6) in 2015–2016, 4.8 (95% *CI*: 3.8, 5.8) in 2017–2018, 5.9 (95% *CI*: 4.8, 7.1) in 2019–2020, and reaching 7.2 (95% *CI*: 4.5, 9.8) per 100 PYs in 2021–2022 (Figure 2). Results from multivariate analysis indicated certain patterns of syphilis risk among MSM. Divorced or widowed MSM had a lower risk compared to those who were unmarried (aHR=0.335, 95% *CI*: 0.142, 0.792). Furthermore, MSM identifying as heterosexual or bisexual exhibited lower risks compared to those identifying as homosexual (aHR=0.605, 95% *CI*: 0.459, 0.964). A rather alarming observation was that MSM who reported using psychoactive substances in the last six months had a 50.4% higher syphilis incidence risk compared to those who reported no use of such substances (aHR=1.504, 95% *CI*: 1.169, 1.934) (Table 2).

DISCUSSION

Our research presents the results of the inaugural long-term cohort study investigating the incidence rate of HIV/syphilis and contributing factors within Tianjin's population. We documented an HIV incidence rate of 2.3 per 100 PYs among MSM in Tianjin. This rate surpasses the one reported in Australia (*8*) yet remains lower than the incidence rate identified in Chengdu city(*9*). Interestingly, the syphilis incidence rate among Tianjin's MSM population (4.75 per 100 PYs) exceeded the rates noted in Australian studies (*10*).

Our study observed a declining incidence of HIV among MSM in Tianjin, contrasting with an upward trend in syphilis incidence. This divergence may be attributed to the comprehensive preventative interventions for MSM that have been in place over recent years. First, mRNA surveillance for acute HIV infection among MSM has been conducted since 2015. Additionally, pooled nucleic acid testing has been employed since 2015 for MSM who initially tested HIV-negative, with the goal of identifying early-stage infections and promptly starting treatment. Measures such as post-exposure prophylaxis (PEP), pre-exposure prophylaxis (PrEP), increased HIV testing coverage through self-testing, volunteer promotion, and advocating for herpes testing before homosexual intercourse have all been introduced. Given that instances of HIV/AIDS transmission via homosexual contact frequently commence antiretroviral treatment punctually (*5*), these efforts have fostered a reduction

TABLE 1. Factors associated with HIV incidence among MSM in Tianjin Municipality, China.

Variables	HIV conversions	PYs	Incidence rate (/100 PYs)	Univariate analysis		Multivariate analysis	
				HR (95% *CI*)	*P* value	*HR* (95% *CI*)	*P* value
Age group (years)							
<20	8	260.4	3.1	1.000		1.000	
20–29	89	3,468.0	2.6	0.835 (0.405, 1.722)	0.625	0.808 (0.381, 1.712)	0.577
30–39	30	1,669.1	1.8	0.587 (0.269, 1.281)	0.181	0.491 (0.211, 1.146)	0.491
≥40	24	1,088.5	2.2	0.726 (0.326, 1.616)	0.433	0.566 (0.229, 1.398)	0.566
Household registration							
Tianjin	68	2,376.8	2.9	1.000		1.000	
Other city	83	4,109.2	2.0	0.712 (0.517, 0.982)	0.038	0.750 (0.530, 1.060)	0.104
Ethnicity							
Ethnic minorities	3	65.1	4.6	1.000		1.000	
Han	148	6,420.9	2.3	0.509 (0.161, 1.604)	0.249	0.649 (0.204, 2.067)	0.464
Marital Status							
Unmarried	111	4,600.6	2.4	1.000		1.000	
Married/cohabiting	31	1,602.7	1.9	0.809 (0.543, 1.206)	0.299	0.974 (0.583, 1.627)	0.920
Divorced/widowed	9	282.7	3.2	1.325 (0.671, 2.614)	0.417	1.378 (0.647, 2.933)	0.405
Education							
Junior high school and below	20	831.2	2.4	1.000		1.000	
High school and above	131	5,654.8	2.3	0.958 (0.598, 1.535)	0.859	0.995 (0.602, 1.646)	0.985
Sexual orientation							
Homosexual	131	5,216.6	2.5	1.000		1.000	
Bisexual/heterosexual	20	1,269.4	1.6	0.633 (0.395, 1.015)	0.058	0.597 (0.358, 0.996)	0.048
Having unprotected anal sex in the last six months							
No	48	2,686.1	1.8	1.000		1.000	
Yes	103	3,799.9	2.7	1.518 (1.078, 2.139)	0.017	1.436 (1.014, 2.033)	0.041
Number of anal intercourse in the last one week							
≤1	131	5,683.8	2.3	1.000		1.000	
≥2	20	802.2	2.5	1.074 (0.671, 1.720)	0.766	1.064 (0.661, 1.713)	0.798
Having commercial homosexual intercourse in the last six months							
No	146	6,124.5	2.4	1.000		1.000	
Yes	5	361.5	1.4	0.585 (0.240, 1.426)	0.238	0.777 (0.314, 1.924)	0.586
Age of first homosexual intercourse (years)							
≤19	61	3,012.0	2.0	1.000		1.000	
≥20	90	3,474.0	2.6	1.282 (0.926, 1.775)	0.134	1.467 (1.023, 2.104)	0.037
Main places to find homosexual partners							
Internet dating software	117	5,041.7	2.3	1.000		1.000	
Other locations	34	1,444.3	2.4	1.019 (0.694, 1.495)	0.923	1.221 (0.817, 1.824)	0.330
Psychoactive substances use							
No	62	3,198.0	1.9	1.000		1.000	
Yes	89	3,288.0	2.7	1.410 (1.019, 1.953)	0.038	1.584 (1.137, 2.207)	0.007
Number of follow-up visits							
≤2	81	1,475.0	5.5	1.000		1.000	
≥3	70	5,011.0	1.4	0.218 (0.154, 0.308)	0.000	0.216 (0.152, 0.308)	0.000
Syphilis infection							
No	129	5,935.3	2.2	1.000		1.000	
Yes	22	550.7	4.0	1.828 (1.163, 2.873)	0.009	1.795 (1.131, 2.849)	0.013

Abbreviation: PYs=person-years; *HR*=hazard ratio.

TABLE 2. Factors associated with the incidence of syphilis among MSM in Tianjin, China.

Variables	Syphilis conversions	PYs	Incidence rate (/100 PYs)	Univariate analysis		Multivariate analysis	
				HR (95% *CI*)	*P* value	*HR* (95% *CI*)	*P* value
Age group (years)							
<20	12	202.5	5.9	1.000		1.000	
20–29	134	3,062.7	4.4	0.737 (0.408, 1.330)	0.310	0.716 (0.391, 1.313)	0.280
30–39	60	1,391.9	4.3	0.733 (0.394, 1.362)	0.326	0.826 (0.424, 1.607)	0.573
≥40	54	812.2	6.6	1.121 (0.600, 2.096)	0.721	1.628 (0.810, 3.271)	0.171
Household registration							
Tianjin	102	2,019.9	5.0	1.000		1.000	
Other city	158	3,449.4	4.6	0.909 (0.709, 1.167)	0.455	0.837 (0.638, 1.098)	0.199
Ethnicity							
Ethnic minorities	3	54.7	5.5	1.000		1.000	
Han	257	5,414.6	4.7	0.840 (0.268, 2.632)	0.765	0.971 (0.308, 3.058)	0.959
Marital Status							
Unmarried	189	3,926.8	4.8	1.000		1.000	
Married/cohabiting	65	1,299.6	5.0	1.048 (0.790, 1.390)	0.744	0.867 (0.603, 1.248)	0.443
Divorced/widowed	6	242.9	2.5	0.522 (0.231, 1.176)	0.117	0.335 (0.142, 0.792)	0.013
Education							
Junior high school and below	36	660.9	5.4	1.000		1.000	
High school and above	224	4,808.4	4.7	0.855(0.601, 1.217)	0.385	0.770 (0.525, 1.129)	0.181
Sexual orientation							
Homosexuality	221	4,380.9	5.0	1.000		1.000	
Bisexual/heterosexual	39	1,088.4	3.6	0.722 (0.513, 1.017)	0.062	0.605 (0.459, 0.964)	0.031
Had unprotected anal sex in the last six months							
No	112	2,282.8	4.9	1.000		1.000	
Yes	148	3,186.5	4.6	0.954 (0.746, 1.219)	0.705	0.952 (0.742, 1.220)	0.697
Number of anal intercourse in the last 1 week							
≤1	222	4,755.2	4.7	1.000		1.000	
≥2	38	714.2	5.3	1.145 (0.811, 1.615)	0.441	1.100 (0.774, 1.562)	0.596
Having commercial homosexual intercourse in the last six months							
No	222	5,199.6	4.3	1.000		1.000	
Yes	38	269.8	14.1	1.195 (0.709, 2.013)	0.504	1.217 (0.711, 2.083)	0.473
Age of first homosexual intercourse (years)							
≤19	126	2,566.6	4.9	1.000		1.000	
≥20	134	2,902.7	4.6	0.939(0.736, 1.198)	0.612	0.964 (0.735, 1.265)	0.793
Main places to find homosexual partners							
Internet dating software	209	4,218.9	5.0	1.000		1.000	
Other locations	51	1,250.5	4.1	0.831 (0.611, 1.130)	0.238	0.787 (0.568, 1.089)	0.148
Psychoactive substances use							
No	108	2,728.7	4.0	1.000		1.000	
Yes	152	2,740.7	5.5	1.414 (1.104, 1.811)	0.006	1.504 (1.169, 1.934)	0.001

Abbreviation: PYs=person-years; *HR*=hazard ratio.

in HIV incidence. Contrastingly, while the Undetectable equals Untransmittable (U=U) theory has spurred increased emphasis on HIV testing and treatment, it has also prompted a surge in syphilis incidence, attributed to the persistence of unregulated unsafe sexual behaviors. Notably, syphilis is known to heighten the risk of HIV infection (*11*), and our findings suggest that MSM infected with syphilis are more likely to seroconvert to HIV. Thus, the higher incidence of syphilis signals an elevated future potential for HIV transmission. Moreover, there is a substantial overlap of HIV and syphilis infection among Asian MSM (*12*). This underlines the need to prioritize screening for and treating sexually transmitted infections (STIs), especially syphilis, as a key strategy for controlling the HIV epidemic. Standardized treatment for those testing positive for syphilis is of paramount importance in preventing its spread and carries broader implications for HIV control. The routine detection of syphilis among HIV/AIDS cases is therefore critical for containing its spread. Consequently, it is vital to integrate HIV and syphilis prevention efforts, and enhance the diagnostic and preventative aspects of syphilis treatment to ensure standardized care.

The use of psychoactive substances, prevalent in 43.5% of MSM in Tianjin (*6*), has been identified as a risk factor contributing to the incidence rates of both HIV and syphilis. It is critical to pay particular attention to MSM who utilize internet dating applications, as the consumption of psychoactive substances is more widespread among this group (*6*). Interestingly, participants identifying as bisexual or heterosexual exhibited lower incidence rates of HIV and syphilis compared to those identifying as homosexual. This variation may be due to a reduced frequency of sexual interactions with other men and differences in sexual roles compared to their homosexual peers. Existing research indicates that homosexual participants are more likely to assume the passive role during anal sex than their bisexual or heterosexual counterparts (*13*), a role that carries an increased susceptibility to contracting HIV/syphilis. Moreover, individuals from this group are more likely to be married to women, and societal and familial pressure may discourage engagement in risky behaviors.

Our findings also revealed that increased age at the time of first homosexual intercourse was linked to a higher risk of HIV, underscoring the significance of implementing targeted education initiatives for older MSM demographics. Regular health check-ups seemed to diminish the risk of HIV, likely due to the heightened healthcare awareness among these individuals.

This study is subject to some limitations. First, tracking the HIV and syphilis status of participants who didn't join the cohort was not possible. Second, our restriction to a cohort of MSM with HIV incidence negated further observation post-HIV conversion, potentially introducing bias into the syphilis incidence data. Yet, despite these constraints, the longevity of the study — spanning a decade — and its exhaustive data set on MSM, offer essential insights into strategies for HIV and syphilis prevention in China's major cities.

In summary, our research points to a steady decline in the incidence of HIV, juxtaposed with a surge in syphilis cases among MSM in Tianjin from 2013 to 2022. We noted sexual orientation and the use of psychoactive substances as shared risk factors for both HIV and syphilis. Our study highlights the difficulties in curbing HIV transmission, largely attributed to the high prevalence of syphilis. This study is of significant value to public health practices intending to prevent HIV and syphilis, underlining the urgency for more robust intervention measures amongst MSM to limit the spread of both HIV and syphilis.

Conflicts of interest: No conflicts of interest.

Acknowledgements: The study participants, data collectors, and the staff from Tianjin Shenlan CBO for their contributions towards quality control.

Funding: Supported by the AIDS Prevention Technical Guidance and Capacity Building Project (No. 102393220020050000012), the Tianjin Medical Key Discipline Project (No. TJYXZDXK-050A), Technical guidance and capacity building for AIDS prevention and control (No. 131031105000160001) and the National Natural Science Foundation of China (No. 72374153).

doi: 10.46234/ccdcw2024.121

[#] Corresponding authors: Houlin Tang, tanghl@chinaaids.cn; Maohe Yu, fish820225@sina.com.

[1] STD & AIDS Control and Prevention Section, Tianjin Center for Disease Control and Prevention, Tianjin, China; [2] National Key Laboratory of Intelligent Tracking and Forecasting for Infectious Diseases, National Center for AIDS/STD Control and Prevention, Chinese Center for Disease Control and Prevention, Beijing, China; [3] STD & AIDS Control and Prevention department, Tianjin Hongqiao District Center for Disease Control and Prevention, Tianjin, China; [4] Tianjin Shenlan Public Health Counseling Service Center, Tianjin, China; [5] Tianjin Key Laboratory of Pathogenic Microbiology of Infectious Disease, Tianjin Centers for Disease Control and Prevention, Tianjin, China.

[&] Joint first authors.

Submitted: December 11, 2023; Accepted: June 28, 2024

REFERENCES

1. Joint United Nations Programme on HIV/AIDS. The path that endsAIDS: UNAIDS Global AIDS Update 2023.2023. https://www.unaids.org/sites/default/files/media_asset/2023-unaids-global-aids-update_en.pdf. [2023-10-7].
2. Stannah J, Soni N, Lam JKS, Giguère K, Mitchell KM, Kronfli N, et al. Trends in HIV testing, the treatment cascade, and HIV incidence among men who have sex with men in Africa: a systematic review and meta-analysis. Lancet HIV 2023;10(8):e528 – 42. https://doi.org/10.1016/S2352-3018(23)00111-X.
3. Zheng SF. The growing threat of China's HIV epidemic. Lancet Public Health 2018;3(7):e311. https://doi.org/10.1016/S2468-2667(18)30098-7.
4. Karanfilian KM, Almohssen AA, Kapila R, Schwartz RA. Malignant syphilis: a new and revised definition. Int J Dermatol 2023;62(3):369 – 75. https://doi.org/10.1111/ijd.16444.
5. Guo Y, Zhao FN, Hou JY, Bai JY. Analyse the timeliness of initiationanti-retroviral treatment among newly diagnosed HIV/AIDS cases in Tianjin, 2016-2020. Chin J AIDS STD 2022;28(1):78 – 81. https://doi.org/10.13419/j.cnki.aids.2022.01.17.
6. Guo Y, Yang J, Bai JY, Liu ZQ, Dong XY, Li L, et al. Analysis on psychoactive substances use in men who have sex with men in Tianjin. Chin J Epidemiol 2022;43(5):686 – 91. https://doi.org/10.3760/CMA.J.CN112338-20211104-00851.
7. Hui S, Chen FF, Li Y, Cui Y, Zhang JH, Zhang L, et al. Factors associated with newly HIV infection and transmitted drug resistance among men who have sex with men in Harbin, P. R. China. Front Public Health 2022;10:860171. https://doi.org/10.3389/fpubh.2022.860171.
8. Grulich AE, Guy R, Amin J, Jin FY, Selvey C, Holden J, et al. Population-level effectiveness of rapid, targeted, high-coverage roll-out of HIV pre-exposure prophylaxis in men who have sex with men: the EPIC-NSW prospective cohort study. Lancet HIV 2018;5(11):e629 – 37. https://doi.org/10.1016/S2352-3018(18)30215-7.
9. You XY, Gilmour S, Cao WN, Lau JTF, Hao C, Gu J, et al. HIV incidence and sexual behavioral correlates among 4578 men who have sex with men (MSM) in Chengdu, China: a retrospective cohort study. BMC Public Health 2021;21(1):802. https://doi.org/10.1186/s12889-021-10835-4.
10. Aung ET, Fairley CK, Ong JJ, Chen MY, Phillips TR, Tran J, et al. Incidence and risk factors for early syphilis among men who have sex with men in Australia, 2013-2019: a retrospective cohort study. Open Forum Infect Dis 2023;10(2):ofad017. https://doi.org/10.1093/ofid/ofad017.
11. Ghanem KG, Ram S, Rice PA. The modern epidemic of syphilis. N Engl J Med 2020;382(9):845 – 54. https://doi.org/10.1056/NEJMra1901593.
12. Mangione CM, Barry MJ, Nicholson WK, Cabana M, Chelmow D, Coker TR, et al. Screening for syphilis infection in nonpregnant adolescents and adults: US preventive services task force reaffirmation recommendation statement. JAMA 2022;328(12):1243 – 9. https://doi.org/10.1001/jama.2022.15322.
13. Xu BY, Aliya A, He Q, Li YF, Ni MJ. HIV infection risk of men who have sex with men with different sex roles. Prev Med 2023;35(12):1018 – 23. https://doi.org/10.19485/j.cnki.issn2096-5087.2023.12.002.

Preplanned Studies

Effectiveness of Frequent Viral Load Testing Plus Additional Interventions to Prevent HIV Transmission in Heterosexual, Serodiscordant Couples — Yunnan Province, China, 2019–2021

Jing Han[1]; Jian Li[1]; Yuhua Shi[2]; Chunpeng Zang[1]; Zhimin Yang[2]; Yu Han[2]; Yanling Ma[2]; Qiongli Duan[3]; Yuhua Hu[4]; Zikuang Bai[5]; Cuiyun Yang[6]; Gabriella Bulloch[7]; Yurong Mao[1]; Houlin Tang[1]; Zunyou Wu[1,†]; Yufen Liu[1,#]

Summary

What is already known about this topic?

HIV transmission among serodiscordant couples remains a persistent issue in China. However, the practice of combining counseling with antiretroviral therapies (ART) to enhance ART adherence is not widely implemented or recommended in Chinese health guidelines.

What is added by this report?

This randomized controlled trial suggests that increased follow-up, counseling, and awareness of HIV risk can enhance ART compliance, thereby maximizing treatment efficacy.

What are the implications for public health practice?

Early testing and counseling of serodiscordant couples, following the identification of a human immunodeficiency virus (HIV) positive spouse, is crucial for initiating ART and reducing the risk of seroconversion in the uninfected partner. Implementing a combination of ART and adjunct counseling in China is advisable.

Approximately two-thirds of newly reported human immunodeficiency virus (HIV) infections in China originate from heterosexual contacts, with one-tenth stemming from a spouse or regular partner (*1*). It is thus crucial to manage transmission within serodiscordant couples to diminish the incidence of new infections. Although the World Health Organization (WHO) underlines the importance of regular viral load monitoring during the early stages of antiretroviral therapies (ART) (*2*), Chinese clinical guidelines currently advise conducting such tests only after six months of ART (*3*). In this study, we enrolled newly diagnosed HIV-1 serodiscordant couples from 15 health centers in Yunnan Province, assigning half to an enhanced prevention strategy. This strategy included a comprehensive reproductive plan, joint spouse testing and consultation, early treatment, frequent viral load monitoring, fertility advice, and ART. The remaining participants received ART alongside the standard care per Chinese guidelines. The enhanced strategy led to a significantly higher number of participants in the intervention group initiating ART within 7 and 14 days of diagnosis compared to the control group. Additionally, the intervention group showed significantly higher rates of viral suppression. None of the spouses in the intervention group were seroconverted (0/100 person-years), while three were in the control group (0.6/100 person-years). These findings support the notion that increased viral load testing frequency and comprehensive counseling can improve treatment outcomes and reduce HIV transmission among serodiscordant couples.

This randomized controlled trial (RCT) recruited HIV-1 serodiscordant couples, all participants being over 18 years of age, from 15 centers in Yunnan Province, China. Inclusion criteria were as follows: the HIV-positive partner was diagnosed during the study period (February 15, 2019 to March 31, 2021); their spouse was confirmed HIV-negative at baseline and maintained this status for three months subsequent to their partner's diagnosis; both partners were aged between 18 and 59 years; the couples consented to participate in the study willingly and were able to provide informed consent; and the couple had engaged in sexual activity at least once in the preceding year. (Data and Sample Collection and HIV-1 Testing refer to the Supplementary Material, available at https://weekly.chinacdc.cn/)

Trained health professionals monitored newly reported positive cases. Couples who met the inclusion

criteria were randomly assigned in a 1:1 ratio to either the intervention group or the standard-of-care group using sequential random grouping.

In the intervention group, health professionals assessed HIV-positive individuals at an outpatient facility, providing treatment consultations and pre-treatment physical examinations. These individuals began ART within one week and underwent viral load testing at 1, 2, 3, 9, 12, and 18 months post-diagnosis. Health professionals also encouraged the HIV-positive patients to disclose their status to their spouses within a week. Couples received counseling on condom usage, HIV care, treatment adherence, reproductive intentions, and safe pregnancy methods. Those planning to conceive were referred to maternal and child health services for expert fertility advice and strategies to prevent perinatal transmission. Viral load results were shared with both partners. The HIV-negative partners underwent testing for HIV seroconversion at 3, 12, 18, and 24 months after the initial HIV diagnosis of their spouses.

In the standard-of-care group, health professionals initiated contact with the treatment facility to commence ART for HIV-positive partners. These partners underwent viral load testing at 3 and 6 months post-diagnosis for comparative analysis with the intervention group. The HIV-negative spouses received testing for HIV seroconversion 3 months after their partners' diagnosis and again at the study's conclusion.

Cox regression was used to estimate relative risks, which were expressed as hazard ratios with 95% confidence intervals (*CI*). A *P* value of less than 0.05 was considered statistically significant. Kaplan-Meier estimates were employed to compare cumulative probabilities of seroconversion between participants in the intervention and control groups. All analyses were conducted using SPSS software (version 24.0, IBM, NewYork, USA).

A total of 2,213 HIV-positive individuals, who either were married or in a committed relationship and aged 18–59, were identified between February 15, 2019, and March 31, 2021, across 15 counties in Yunnan province, China (Figure 1). Of these, 1,470 couples were excluded due to not being serodiscordant or unreachable (n=1,469), or because one partner died within 3 months of diagnosis (n=1). By the close of enrollment on March 31, 2021, 743 couples remained, with 372 assigned to the intervention group and 371 to the control group (Figure 1). Within the intervention group, six couples withdrew due to divorce. In the control group, adverse outcomes included seroconversion in three couples and withdrawals due to divorce (three couples), death of the HIV-positive spouse (three couples), and one couple's decision to cease participation. The duration of observation for those who withdrew did not significantly differ between the groups (P=0.808). (Eligibility flow diagram for HIV serodiscordant couples refer to Supplementary Figure S1, available at https://weekly.chinacdc.cn/)

At enrollment, the majority of participants were male farmers with primary school education. The age of the HIV-positive spouse differed significantly between groups, although other demographic characteristics did not (Table 1). The median observation period was 15.3 (10.8–18.8) person-months for the intervention group and 15.8 (10.6–20.5) person-months per couple for the control group. Significantly more participants in the intervention group initiated ART within 7 and 14 days from diagnosis (P=0.011 and P<0.001, respectively). The median time from diagnosis to initiating ART was 5 days [inter-quartile range (IQR): 2–9] in the intervention group and 6 days (IQR: 2–18) in the control group (Table 2). Rates of achieving a viral load of <1,000 copies/L and <200 copies/L within 3 and 4 months of diagnosis were significantly higher in the intervention group (86.2% and 64.5%; 91.9%, and 75.3%, respectively) compared to the control group (56.3% and 43.1%; 82.8%, and 67.0%). Among those who underwent viral load testing, rates of obtaining viral loads of <1,000 copies/L, <200 copies/L, and <50 copies/L were significantly higher in the intervention group (97.8%, 94.4%, and 90.1%, respectively) compared to the control group (93.9%, 89.0%, and 81.8%) (P<0.05) (Figure 1).

Among HIV-negative spouses at baseline, the seroconversion rates were 0.6 per 100 person-years (3/371) in the control group and 0 per 100 person-years in the intervention group (P=0.081). (Assessment of Linkage of Seroconversions and Analysis of seroconversion case sequences refer to Supplementary Figures S2–S3, available at https://weekly.chinacdc.cn/)

Characteristics of the seroconverted spouses are summarized. (Characteristics of the three seroconverted couples refer to the Supplementary Table S1, available at https://weekly.chinacdc.cn/) The time intervals from the diagnosis of HIV-positive status to spouse seroconversion were 117, 121, and

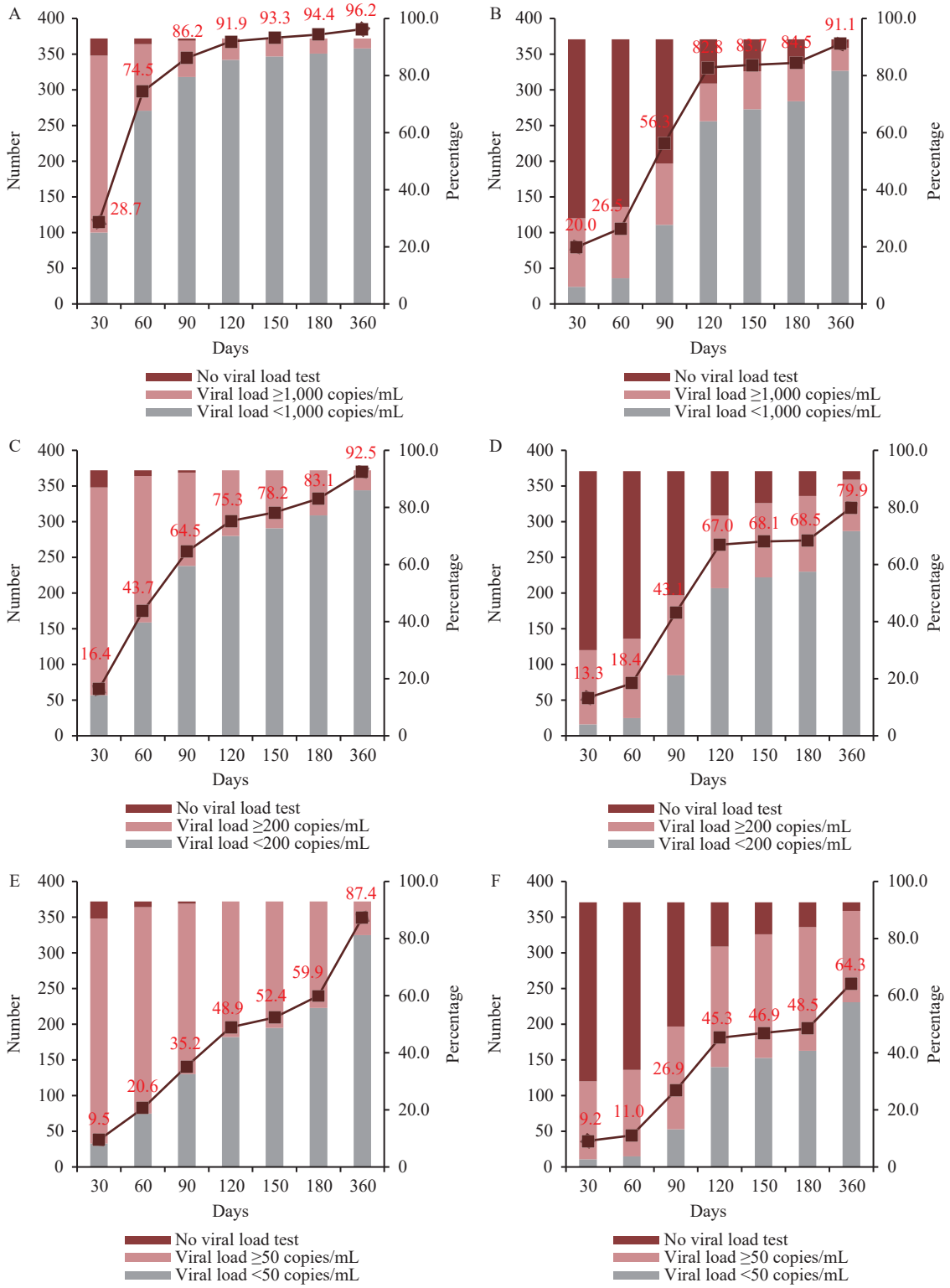

FIGURE 1. Viral suppression iin intervention group and standard-of-care group. (A) VL <1000 copies/mL in intervention group; (B) VL <1000 copies/mL in standard-of-care group; (C) VL <200 copies/mL in intervention group; (D) VL <200 copies/mL in standard-of-care group; (E) VL <50 copies/mL in intervention group; (F) VL <50 copies/mL in standard-of-care group.

182 days, respectively. Phylogenetic analysis confirmed that all seroconversion cases were linked to their HIV-positive partners (refer to Supplementary Figure S2).

DISCUSSION

After 18 months, seroconversion was observed in

TABLE 1. Baseline characteristics of participants in the intervention and control groups.

Variables	Control group participants, *N* (%)	Intervention group participants, *N* (%)	*P* value*
Overall	371 (100.0)	372 (100.0)	
Age, years			
18–39	132 (35.6)	163 (43.8)	0.022
40–59	239 (64.4)	209 (56.2)	
Sex			
Male	250 (67.4)	266 (71.5)	0.223
Female	121 (32.6)	106 (28.5)	
Education			
Illiterate	47 (12.7)	54 (14.5)	0.598
Primary school	175 (47.2)	176 (47.3)	
Junior high school	107 (28.8)	110 (29.6)	
≥Senior high school	42 (11.3)	32 (8.6)	
Occupation			
Farmer	299 (80.6)	311 (83.6)	0.301
Labourer	31 (8.4)	34 (9.1)	
Homemaker/unemployed	26 (7.0)	15 (4.0)	
Others	15 (4.0)	12 (3.2)	
$CD4^+$ T cell count at diagnosis			
≤200	113 (31.1)	119 (32.8)	0.703
201–499	200 (55.1)	189 (52.1)	
≥500	50 (13.8)	55 (15.2)	
Sexual behavior in the past month			
Had sexual behavior			
No	94 (25.3)	67 (18.0)	0.015
Yes	277 (74.7)	305 (82.0)	
Frequency of sexual behaviors			
≤3	162 (58.5)	166 (54.4)	0.324
≥4	115 (41.5)	139 (45.6)	
Frequency of condom use			
Every time	50 (12.5)	24 (8.7)	0.516
Sometimes	131 (32.7)	68 (24.5)	
Never	401 (68.9)	185 (66.8)	

* Categorical variables and continuous variables were compared between the intervention group and the control group using the Chi-square test and T-test, respectively.

three couples from the standard-of-care group, whereas no seroconversions occurred in the intervention group; however, this difference was not statistically significant. Nevertheless, the reduced viral load titers observed in the intervention group suggest that integrating ART with viral load monitoring and non-medical preventative strategies may enhance ART adherence and reduce the likelihood of HIV transmission between spouses.

All three spouses seroconverted within 6 months of initiating ART, aligning with previous findings that this period represents the highest risk for serodiscordant couples starting ART (*4*). This increased vulnerability is attributed to the initial inability of ART to sufficiently suppress viral load, coupled with the persistence of unprotected sexual activities that may facilitate HIV transmission between spouses (*5–6*). Consequently, enhancing provider-

TABLE 2. Follow-up characteristics of participants in the intervention and control groups.

Variables	Control group participants, *N* (%)/median (IQR)	Intervention group participants *N* (%)/median (IQR)	*P* value*
Overall, *N* (%)	371 (100.0)	372 (100.0)	
Seroconversion			
N/100PY	3/486.7 (0)	0/470.8 (0.6)	0.081
Observation time, person-month			
Median (IQR)	15.8 (10.6–20.5)	15.3 (10.8–18.8)	0.227
Days from diagnosis to spouse test			
Median (IQR)	0 (0–4)	0 (0–3)	0.376
Days from diagnosis to ART initiation			
Median (IQR)	6 (2–18)	5 (2–9)	<0.001
Frequency of viral load test			
Median (IQR)	2 (2–3)	7 (5–8)	<0.001
Initiated ART within 7 days from diagnosis, *N* (%)			
No	150 (40.4)	117 (31.5)	0.011
Yes	221 (59.6)	255 (68.5)	
Initiated ART within 14 days from diagnosis, *N* (%)			
No	106 (28.6)	54 (14.5)	<0.001
Yes	265 (71.4)	318 (85.5)	
Sexual behavior in the past month at last recorded follow-up			
Had sexual behavior			
No	129 (34.8)	119 (31.9)	0.421
Yes	242 (65.2)	253 (68.0)	
Frequency of sexual behaviors			
≤3	157 (64.9)	161 (63.6)	0.774
≥4	85 (35.1)	92 (36.4)	
Frequency of condom use during sexual activity			
Sometimes/never	19 (7.9)	10 (4.0)	0.065
Every time	223 (92.1)	243 (96.0)	
Within 3 months after diagnosis			
Viral load test, *N* (%)			
No	174 (46.9)	3 (0.8)	<0.001
Yes	197 (53.1)	369 (99.2)	
Viral load <1,000 copies/L, *N* (%)			
No	86 (43.7)	51 (13.8)	<0.001
Yes	111 (56.3)	318 (86.2)	
Viral load <200 copies/L, *N* (%)			
No	112 (56.9)	131 (35.5)	<0.001
Yes	85 (43.1)	238 (64.5)	
Viral load <50 copies/L, *N* (%)			
No	144 (73.1)	239 (64.8)	0.044
Yes	53 (26.9)	130 (35.2)	

Continued

Variables	Control group participants, *N* (%)/median (IQR)	Intervention group participants *N* (%)/median (IQR)	*P* value*
Within 4 months after diagnosis			
Viral load test, *N* (%)			
No	62 (16.7)	0 (0)	<0.001
Yes	309 (83.3)	372 (100.0)	
Viral load <1,000 copies/L, *N* (%)			
No	53 (17.2)	30 (8.1)	0.001
Yes	256 (82.8)	342 (91.9)	
Viral load <200 copies/L, *N* (%)			
No	102 (33.0)	92 (24.7)	0.017
Yes	207 (67.0)	280 (75.3)	
Viral load <50 copies/L, *N* (%)			
No	169 (54.7)	190 (51.1)	0.347
Yes	140 (45.3)	182 (48.9)	
Viral load at last recorded follow-up			
Viral load test, *N* (%)			
No	8 (2.2)	0 (0)	0.004
Yes	363 (97.8)	372 (100.0)	
Viral load <1,000 copies/L, *N* (%)			
No	22 (6.1)	8 (2.2)	0.007
Yes	341 (93.9)	364 (97.8)	
Viral load <200 copies/L, *N* (%)			
No	40 (11.0)	21 (5.6)	0.008
Yes	323 (89.0)	351 (94.4)	
Viral load <50 copies/L, *N* (%)			
No	66 (18.2)	37 (9.9)	0.001
Yes	297 (81.8)	335 (90.1)	

Abbreviation: IQR=inter-quartile range.
* Categorical variables and continuous variables were compared between the intervention group and the control group using the Chi-square test and T-test, respectively.

patient communication regarding the high likelihood of seroconversion during the initial six months of ART and emphasizing the necessity of adherence could serve as crucial strategies. These measures are essential not only for educating on safer sexual practices but also for achieving viral suppression as swiftly as possible (*7*).

Although no statistical differences were identified between groups, seroconversion rates were notably lower compared to similar populations documented in other Chinese studies from Yunnan (*8*–*9*). For the intervention groups, the low incidence of seroconversion could be attributed to stringent testing and counseling. However, the awareness associated with enrolling in an unblinded RCT might introduce selection bias and increase motivation among both groups to engage in health-promoting behaviors (*10*).

Although this study offers insights into the impact of supplementary preventative strategies on HIV seroconversion, several limitations must be acknowledged. Given the non-blinded nature of this study, participants in the standard-of-care group were aware that they were not receiving additional interventions. This awareness may have engendered feelings of disadvantage, potentially prompting more cautious behaviors that could reduce seroconversion rates and introduce bias; however, this effect is presumed to be minimal. The absence of statistical significance between groups suggests that both

intensive and non-intensive preventative strategies are effective, provided that ART is recommended and adhered to. Nevertheless, the sample size and follow-up durations were suboptimal compared to other studies, implying a need for optimization to confidently and safely conclude that extensive viral load monitoring and additional preventative measures do not further reduce the risk of seroconversion. Additionally, the study's restriction to a single province in China might limit its generalizability to other regions with different cultural and demographic profiles, which could affect adherence to and acceptance of HIV and ART protocols. Despite a solid foundation in HIV/Acquired Immune Deficiency Syndrome (AIDS) prevention and control efforts in Yunnan Province, the lack of interventions in the control group might still influence the outcomes due to overarching prevention activities. Future studies that employ blinding, larger cohorts, and extended follow-up durations may yield more definitive conclusions on whether the standard-of-care guidelines in China are as effective as multiple intervention strategies.

Ethics approval and consent to participate: The protocol was reviewed approved by the Institutional Review Board of National Center for AIDS/STD Control and Prevention, Chinese Center for Disease Control and Prevention (Project No: X190111538) and was registered on Chinese Clinical Trail Register (RegistrationNo: ChiCTR1900021192). All participants signed informed consent before enrolling in the study.

Conflicts of interest: No conflicts of interest.

Funding: Funding The study was supported by the National Health Commission of the People's Republic of China (grant number 2018ZX10721102).

doi: 10.46234/ccdcw2024.122

[#] Corresponding author: Yufen Liu, yufenliu69@chinaaids.cn.

[1] National Center for AIDS/STD Control and Prevention, Chinese Center for Disease Control and Prevention, Beijing, China; [2] Yunnan Provincial Center for Disease Control and Prevention, Kunming City, Yunnan Province, China; [3] Honghe Prefectural Center for Disease Control and Prevention, Honghe City, Yunnan Province, China; [4] Wenshan Prefectural Center for Disease Control and Prevention, Wenshan City, Yunnan Province, China; [5] Zhaotong Prefectural Center for Disease Control and Prevention, Zhaotong City, Yunnan Province, China; [6] Lincang Prefectural Center for Disease Control and Prevention, Lincang City, Yunnan Province, China; [7] Faculty of Medicine, Dentistry and Health Sciences, University of Melbourne, Melbourne, VIC, Australia.

[†] Deceased author.

Submitted: December 29, 2023; Accepted: July 01, 2024

REFERENCES

1. Wang LY, Ding ZW, Qin QQ, Cai C, Guo W, Cui Y. Characteristics of HIV transmission through heterosexual contact in China, 2008-2014. Chin J Epidemiol 2015;12(12):1332 – 6. https://doi.org/10.3760/cma.j.issn.0254-6450.2015.12.002.
2. Glass T, Myer L, Lesosky M. The role of HIV viral load in mathematical models of HIV transmission and treatment: a review. BMJ Glob Health 2020;5(1):e001800. https://doi.org/10.1136/bmjgh-2019-001800.
3. Ministry of Health Working Group on Clinical AIDS Treatment. China free antiretroviral treatment manual. 4th ed. Beijing: People's Medical Publishing House. 2016. https://www.docin.com/p-2355721091.html&key=%E8%89%BE%E6%BB%8B%E7%97%85%E6%80%8E%E4%B9%88%E6%B2%BB. (In Chinese).
4. Mujugira A, Celum C, Coombs RW, Campbell JD, Ndase P, Ronald A, et al. HIV transmission risk persists during the first 6 months of antiretroviral therapy. J Acquir Immune Defic Syndr 2016;72(5):579 – 84. https://doi.org/10.1097/QAI.0000000000001019.
5. Jia ZW, Mao YR, Zhang FJ, Ruan YH, Ma Y, Li J, et al. Antiretroviral therapy to prevent HIV transmission in serodiscordant couples in China (2003-11): a national observational cohort study. Lancet 2013;382(9899):1195 – 203. https://doi.org/10.1016/S0140-6736(12)61898-4.
6. Baggaley RF, White RG, Hollingsworth TD, Boily MC. Heterosexual HIV-1 infectiousness and antiretroviral use: systematic review of prospective studies of discordant couples. Epidemiology 2013;24(1):110 – 21. https://doi.org/10.1097/EDE.0b013e318276cad7.
7. Baker Z, Gorbach P, De Melo MG, Varela I, Sprinz E, Santos B, et al. The effect of partnership presence and support on HIV viral suppression among serodiscordant partnered and single heterosexual HIV-positive individuals in Brazil. AIDS Behav 2021;25(6):1946 – 53. https://doi.org/10.1007/s10461-020-03124-5.
8. Wang L, Peng Z, Li M, Norris J, Wang L, Cao W, et al. HIV seroconversion and prevalence rates in heterosexual discordant couples in China: a systematic review and meta-analysis. AIDS Care, 2012;24:1059 – 70
9. Tang HL, Wu ZY, Mao YR, Cepeda J, Morano J. Risk factor associated with negative spouse HIV seroconversion among sero-different couples: a nested case-control retrospective survey study in 30 counties in Rural China. PLoS One 2016;11(10):e0164761. https://doi.org/10.1371/journal.pone.0164761.
10. Lewis SC, Warlow CP. How to spot bias and other potential problems in randomised controlled trials. J Neurol, Neurosurg Psychiatry 2004;75(2):181 – 7. https://doi.org/10.1136/jnnp.2003.025833.

SUPPLEMENTARY MATERIAL

Assessment of Linkage of Seroconversions

When the HIV-negative partner tested positive, an initial questionnaire survey was conducted to determine if the infection originated from the HIV-positive spouse. Samples from both spouses were collected and analyzed at a laboratory within the Yunnan Province Center for Disease Control and Prevention (CDC) to genetically assess whether seroconversion occurred due to the spouse. HIV-1 gag gene sequences were generated through population sequencing for the study-partner pairs, as well as for 10 additional HIV-infected local control subjects from the same county site.

RNA extraction, Reverse Transcription Polymerase Chain Reaction (RT-PCR) amplification, and nucleotide sequencing were conducted in physically distinct laboratories. Viral RNA was extracted utilizing the Viral RNA Extraction Mini Kit (QIAGen, Hilden, Germany). The extracted RNA was then reverse-transcribed into cDNA, serving as the template for PCR amplification of the HIV-1 pol gene via nested PCR (Takara Biotechnology, China). Subsequently, the PCR products were sequenced using the ABI PRISM 3730XL DNA Analyzer (Applied Biosystems, USA).

Phylogenetic methods were employed to analyze the sequences. MEGA software version 11.0 facilitated phylogenetic and molecular evolutionary analyses. The likelihood of linkage was evaluated using Bayes' theorem, comparing the genetic similarity of HIV-1 among partner pairs to that among local control subjects. Phylogenetic dendrograms were generated through the neighbor-joining method, employing Kimura two-parameter modeling, and node reliability was assessed by bootstrapping with 1,000 replicates.

Data and Sample Collection

At each baseline and follow-up visit, couples participating in the study were interviewed face-to-face by a trained public health professional using a standardized questionnaire. During the baseline assessment, HIV-positive spouses provided information about their demographic characteristics, routes of HIV transmission, sexual practices with their HIV-negative partners over the past month, condom usage frequency, and fertility intentions. Subsequent follow-up visits included additional queries about medication adherence and any instances of missed doses for the HIV-positive spouses. To monitor health indicators, 7 mL and 5 mL of venous blood were collected from HIV-positive individuals for viral load testing and $CD4^+$ T cell count analysis, respectively. For HIV-negative spouses, 5 mL of blood was drawn for HIV testing. In cases of seroconversion, genetic and phylogenetic analyses were conducted using blood samples from both spouses.

HIV-1, CD4 and Viral Load Testing

HIV testing was conducted using either a commercially available ELISA or a rapid test. Samples that tested positive were subsequently confirmed through an alternative strategy employing four rapid tests. $CD4^+$ T cell counts were quantified using flow cytometers from Agilent, USA. HIV viral load was determined with the COBAS AmpliPrep/COBAS TaqMan HIV-1 Test, version 2.0 (Branchburg, USA), which features a lower detection limit (LDL) of 20 copies/mL. All procedures were carried out following the manufacturer's instructions.

SUPPLEMENTARY TABLE S1. Characteristics of the three seroconverted couples

Characteristics	Subject 1	Subject 2	Subject 3
Variables of seroconverted spouse			
Age (years)	41	50	53
Gender	Male	Male	Female
Education	Illiterate	Illiterate	Primary school
Days from last HIV negative test to HIV positive test	117	112	81
Days from HIV positive spouse diagnosis to seroconversion test	117	121	172
Unprotected sexual behavior with spouse within 3 months before seroconversion testing	13	10	2
First $CD4^+$ T cell count	364	495	343
Variables of HIV-positive spouse (index cases)			
Age (years)	41	56	43
Gender	Female	Female	Male
Education	Illiterate	Illiterate	Primary school
Viral load at enrollment	–	1,170,000	–
Viral load at 3 months of diagnosis	632	2,070	<20
Days from diagnosis to ART initiation	7	21	13
First $CD4^+$ T cell count	337	228	169

Abbreviation: HIV=human immunodeficiency virus.
"–"means did not receive viral load test at enrollment.

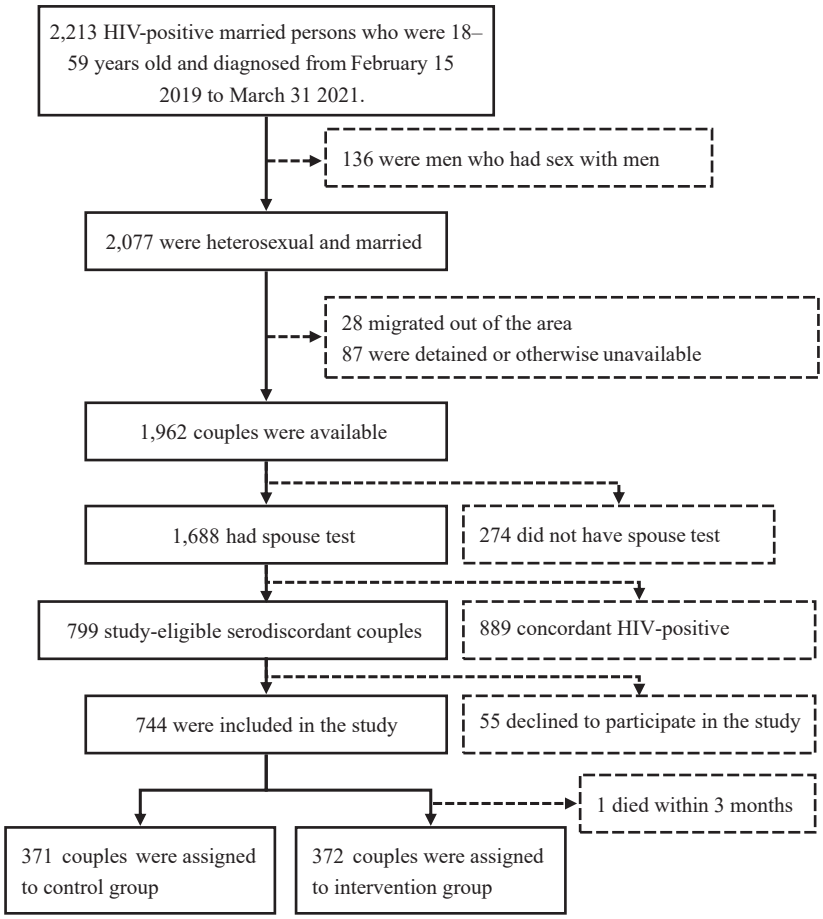

SUPPLEMENTARY FIGURE S1. Eligibility flow diagram for HIV serodiscordant couples.
Note: During the study period, a total of 2,213 participants diagnosed as HIV-positive were initially considered. However, 1,469 couples were excluded due to either not being serodiscordant or being unreachable, and one HIV-positive participant passed away from AIDS-related diseases within three months of diagnosis. Consequently, at the end of the enrollment phase, the study included 743 couples, with 372 couples assigned to the intervention group and 371 to the control group.
Abbreviation: HIV=human immunodeficiency virus.

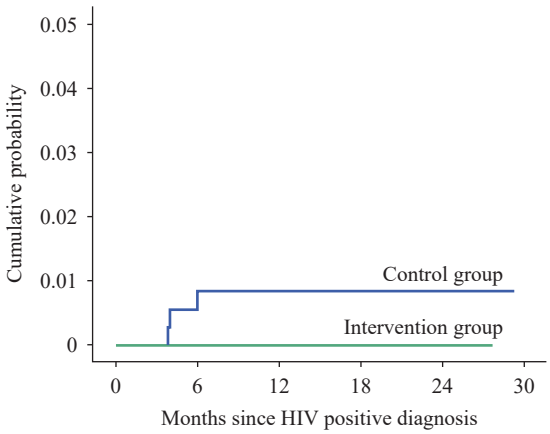

SUPPLEMENTARY FIGURE S2. Kaplan-Meier estimates for the cumulative probabilities of seroconversion among participants in the intervention and control groups.
Abbreviation: HIV=human immunodeficiency virus.

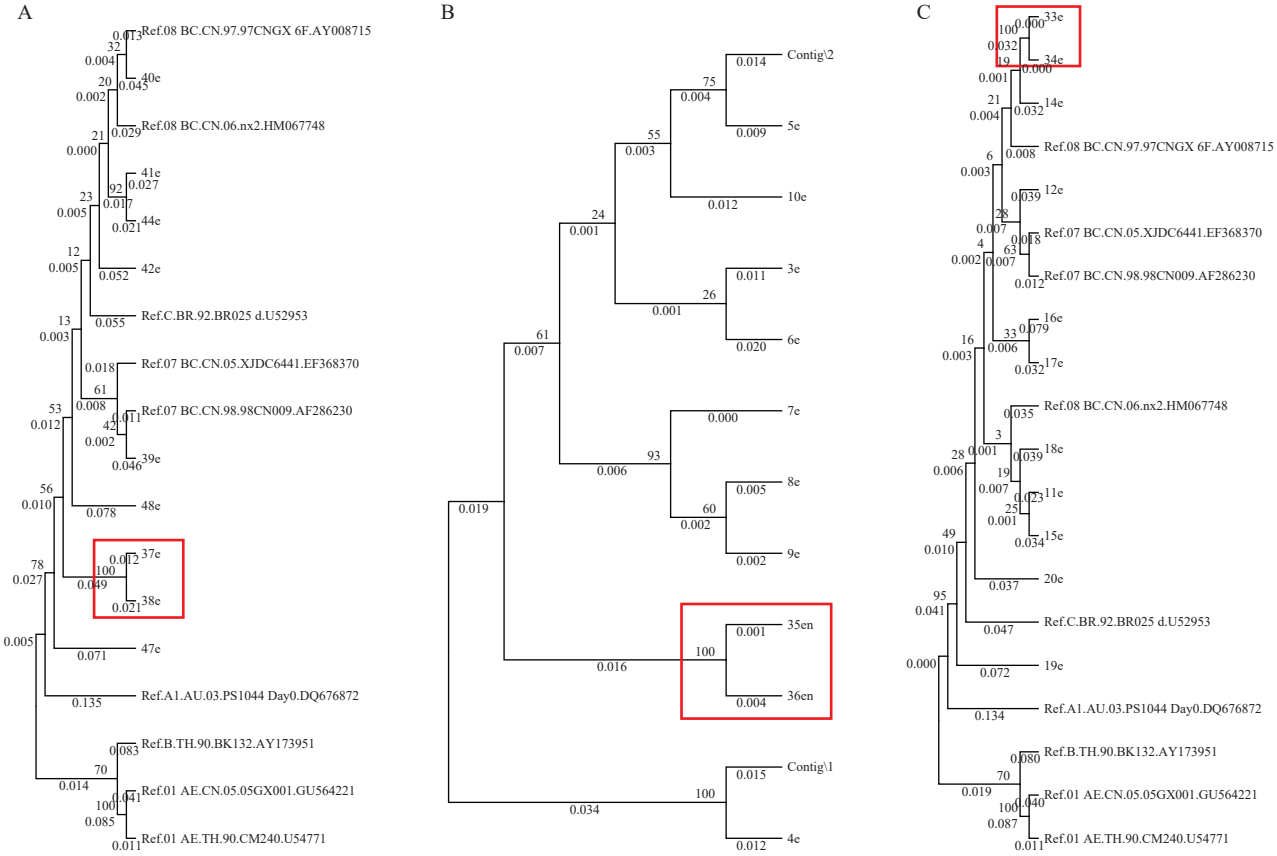

SUPPLEMENTARY FIGURE S3. Analysis of seroconversion case sequences. (A) Seroconversion couple 37e and 38e HIV DNA sequence analysis; (B) Seroconversion couple 35en and 36en HIV DNA sequence analysis; (C) Seroconversion couple 33e and 34e HIV DNA sequence analysis.

Vital Surveillances

The Epidemiological Characteristics and Spatiotemporal Clustering of Measles — China, 2005–2022

Qianqian Liu[1]; Jiuhong Li[1]; Siyu Liu[1]; Lin Tang[1]; Xiaoqi Wang[1]; Aodi Huang[1]; Xia Xu[1]; Yuexin Xiu[1]; Hong Yang[1]; Ning Wen[1]; Lance Rodewald[1]; Fuzhen Wang[1]; Zundong Yin[1,#]

ABSTRACT

Introduction: In recent years, the incidence of measles in China has consistently remained below 1 per 100,000 population, yet the disease has not been eliminated. This study aims to comprehensively analyze the epidemiological characteristics of measles from 2005 to 2022, identify high-risk populations and areas, and propose targeted interventions.

Methods: We utilized data from the China Disease Prevention and Control Information System for our comprehensive analysis. Spatial autocorrelation was employed to examine the spatial clustering of measles, while spatiotemporal scanning analysis was used to detect spatiotemporal clustering to describe measles epidemiology during the study period.

Results: Between 2005 and 2022, 732,218 measles cases were reported in China. Overall, the incidence of measles exhibited a downward trend, particularly during the periods of 2008–2011 and 2015–2022. In 2022, the incidence rate reached its historical low at 0.039 per 100,000 population. Measles predominantly affects young children. Since 2017, global spatial clustering has diminished, although hotspot areas persist in the western provinces. Spatial-temporal scanning identified a high-incidence cluster from 2005 to 2008, comprising 15 provinces in the western, central, and northern regions of China. Conversely, from 2016 to 2022, a low-incidence cluster was detected in the southern and central provinces.

Conclusions: China has made significant progress in measles prevention and control. The recent low incidence and absence of substantial spatiotemporal clustering indicate that China is nearing measles elimination. However, there is a continuing need to enhance prevention and control efforts among very young children and in historic incidence hotspots in western provinces. Additionally, improving the diagnosis of vaccine-associated rash illnesses is essential.

Measles is an acute, highly contagious viral disease characterized by fever, rash, cough, conjunctivitis, and coryza. The measles virus is extremely transmissible, with over 90% of susceptible individuals developing symptoms upon exposure. Historically, measles has been one of the most common acute respiratory infections in children, with significant outbreak potential (*1*). Global efforts have been directed towards eliminating measles. In 2020, the World Health Organization (WHO) introduced the "2021–2030 Global Measles and Rubella Strategic Framework," which aims to achieve and sustain regional measles elimination by 2030 (*2*). Vaccination with measles-containing vaccines (MCV) remains the most cost-effective and efficient method for preventing measles and its complications. Since the implementation of planned immunization in China in 1978, the incidence of measles has dramatically decreased. From 2017 onwards, the reported incidence rate of measles in China has been below 1 per 100,000, indicating progress towards the elimination goal (*3*–*5*). This study analyzes the epidemiological characteristics and spatiotemporal distribution of measles in China from 2005 to 2022 to provide a scientific basis for enhancing measles prevention and control measures.

METHODS

We obtained measles reporting data from the China Disease Prevention and Control Information System to assess the epidemiological characteristics of measles based on the date of illness onset. All clinical diagnostic cases and laboratory-confirmed cases reported between 2005 and 2022 were included in our study. Incidence was calculated as the number of reported cases divided by the population size for that year, excluding Hong Kong Special Administrative Region (SAR); Macao SAR; and Taiwan, China.

We constructed an analytical database using Microsoft Excel 2019 (version 2019, Microsoft Corporation, Redmond, WA, USA) and applied joinpoint regression to evaluate trends in incidence with the Joinpoint Regression Program (version 4.9, Information Management Services, Inc., Calverton, MD, USA) by Kim and colleagues (*6*). Spatial autocorrelation was assessed using Moran's I statistic in ArcGIS Desktop (version 10.6, Environmental Systems Research Institute Inc., California, USA). To identify provincial-level disease hotspots, we employed the Getis-Ord Gi* index (*7*). A region and its surrounding areas were considered significant hotspots if they exhibited higher values according to the index. We utilized the space-time scan statistic in SaTScan (version 9.6, Information Management Services, Maryland, USA), based on spatial dynamic window scanning, to investigate the spatial-temporal clustering of measles (*8*). Statistical significance was determined with a threshold (α) set at 0.05, with *P* values less than 0.05 considered significant.

RESULTS

From 2005 to 2022, a total of 732,218 measles cases were reported in China, comprising 431,053 males and 301,165 females, resulting in a male-to-female ratio of 1.43:1. The incidence rate varied from 0.039 to 9.95 per 100,000, with an average reported incidence of 3.00 per 100,000 (Figure 1). Joinpoint regression identified three incidence inflection points in 2008, 2011, and 2015. The annual percentage changes (APC) for the periods 2005–2008, 2008–2011, 2011–2015, and 2015–2022 were 2.13 [95% confidence interval (*CI*): −8.09, 22.52, *P*>0.05], −51.17 (95% *CI*: −62.35, −37.01, *P*<0.05), 37.59 (95% *CI*: 13.05, 109.94, *P*<0.05), and −55.28 (95% *CI*: −73.83, −44.01, *P*<0.05), respectively. The average annual percentage change (AAPC) was −31.55 (95% *CI*: −43.03, −27.12, *P*<0.05). Overall, the reported incidence of measles showed a significant decline from 2005 to 2022, with notable reductions during the periods 2008–2011 and 2015–2022.

Measles cases were reported monthly throughout the study period. Significant seasonal peaks in measles incidence were observed from 2005 to 2010 and again from 2013 to 2016, predominantly occurring between March and June. However, starting in 2017, the seasonality became less distinct, with cases reported sporadically year-round. The highest incidence was observed in the 0–4 year age group at 26.03 per 100,000, followed by the 5–9 year age group at 6.21 per 100,000. Among children under ten years, infants had the highest incidence at 75.41 per 100,000 (Figure 2). Overall, the majority (51.18%) of measles cases were in children under 5 years old, with very few cases in adults aged 50 years and older, excluding 14 cases with unknown ages.

The global spatial autocorrelation analysis of measles incidence rates from 2005 to 2022 revealed that Moran's *I* values varied between −0.14 and 0.55. Significant spatial clustering of measles was identified during 2010–2011 and 2014–2017, with Moran's *I* values over 0 and statistically significant (*P*<0.05). Local spatial autocorrelation analysis indicated that the number of provincial-level administrative divisions (PLADs) with measles hotspots ranged from zero to

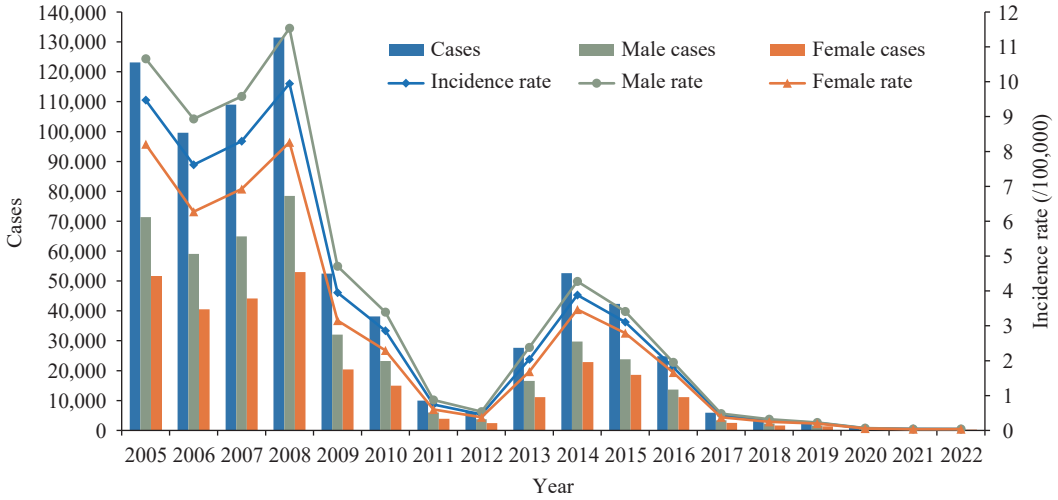

FIGURE 1. Measles reported cases and incidence rates in China from 2005 to 2022.

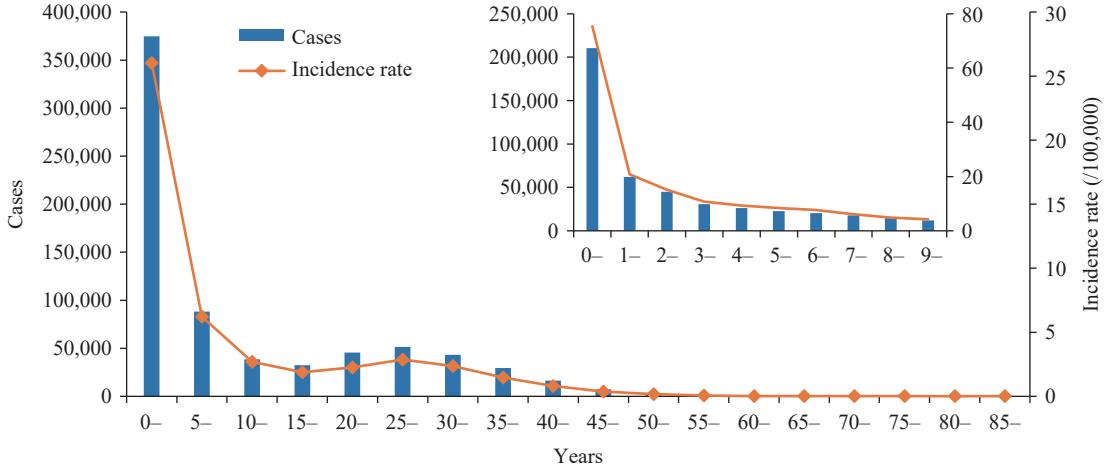

FIGURE 2. Measles reported cases and incidence rates by age group in China from 2005 to 2022.

five (P<0.05). Hotspots were predominantly found in western PLADs. Although the overall measles incidence decreased to less than 1/100,000 in 2017 and no global spatial clustering was observed subsequently, incidence hotspots were still detected in western PLADs through local spatial autocorrelation analysis. Only one cold spot was detected in Yunnan in 2009 (Table 1). Spatiotemporal scan analysis identified one high-risk cluster and one low-risk cluster, encompassing 15 and 13 provincial-level areas, respectively (Table 2). The high-risk cluster persisted from 2005 to 2008 [relative risk (*RR*) =4.69, log-likelihood ratio (*LLR*) =140,816, P<0.001)], while the low-risk cluster persisted from 2016 to 2022 (*RR*=0.08, *LLR*=113,675, P<0.001).

DISCUSSION

Our study demonstrated a decline in the overall incidence of measles in China from 2005 to 2022, with the most significant reductions occurring during 2008–2011 and 2015–2022. In recent years, spatial clustering of measles has become considerably less evident.

Vaccination is a fundamental measure for measles eradication. In addition to maintaining high routine immunization coverage, China has conducted multiple rounds of supplementary immunization activities (SIAs) for children aged 8 months to 14 years, tailored to the epidemiology of each province. A unified nationwide SIA was implemented in 2010 to address immunization gaps (*3*,*9*). Following these efforts, the measles incidence in China exhibited a rapid decline during 2008–2011. Furthermore, China has incorporated sensitive and high-quality epidemiological and laboratory-based surveillance as key components of its comprehensive measles elimination strategy. Despite periodic fluctuations, measles incidence decreased consistently from 2015 to 2022.

In recent years, amidst a resurgence in global measles outbreaks (*10*–*11*), China has maintained high coverage with two doses of MCV. Immunization programs at all levels have made significant efforts to vaccinate children who missed their doses during the coronavirus disease 2019 (COVID-19) pandemic, preventing the accumulation of susceptible populations. As a result of these proactive measures, the COVID-19 pandemic has not led to an increase in measles incidence in China (*12*). Furthermore, non-pharmaceutical interventions implemented during the COVID-19 pandemic may have indirectly reduced measles transmission, supporting efforts toward measles elimination. In 2022, China achieved its lowest recorded incidence of measles, indicating substantial progress toward elimination.

Challenges remain in the quest to eliminate measles. Throughout the analysis period, hotspots were predominantly concentrated in western provinces, particularly in Xinjiang, Xizang and Qinghai. This trend suggests that although measles does not cluster nationwide, incidence rates are higher in western China compared to other regions. Western China's vast territories, complex terrains, and large catchment areas for primary immunization services present logistical challenges for vaccine cold chain transportation and storage. These difficulties may undermine routine immunization programs and lead to renewed measles transmission (*13*). To address this, efforts should focus on enhancing primary immunization service capacity and strengthening weak

TABLE 1. Hot and cold spots of measles incidence in China from 2005 to 2022.

Year	Hotspot regions		Cold spot regions	
	N	PLADs	*N*	PLADs
2005	3	Xinjiang, Xizang, Qinghai	0	
2006	0		0	
2007	0		0	
2008	2	Xinjiang, Qinghai	0	
2009	0		1	Yunnan
2010	3	Beijing, Tianjin, Hebei	0	
2011	4	Xinjiang, Xizang, Qinghai, Sichuan	0	
2012	1	Xizang	0	
2013	2	Xinjiang, Xizang	0	
2014	5	Hebei, Beijing, Jilin, Liaoning Tianjin	0	
2015	4	Xinjiang, Xizang, Qinghai, Sichuan	0	
2016	4	Xinjiang, Xizang, Qinghai, Gansu	0	
2017	5	Xinjiang, Xizang, Qinghai, Sichuan, Yunnan	0	
2018	1	Xizang	0	
2019	4	Xinjiang, Xizang, Qinghai, Sichuan	0	
2020	5	Xinjiang, Xizang, Qinghai, Gansu, Sichuan	0	
2021	5	Xinjiang, Xizang, Qinghai, Gansu, Sichuan	0	
2022	5	Xinjiang, Xizang, Qinghai, Gansu, Sichuan	0	

Abbreviation: PLADs=provincial-level administrative divisions.

TABLE 2. Spatiotemporal scan analysis of measles incidence in China from 2005 to 2022.

Cluster types	Year	PLADs
High-prevalence cluster areas	2005–2008	Xinjiang, Qinghai, Xizang, Gansu, Ningxia, Inner Mongolia, Sichuan, Shaanxi, Shanxi, Chongqing, Hebei, Beijing, Henan, Yunnan, Tianjin.
Low-prevalence cluster areas	2016–2022	Guangxi, Hainan, Guizhou, Guangdong, Yunnan, Hunan, Chongqing, Sichuan, Jiangxi, Hubei, Fujian, Shaanxi, Anhui.

Abbreviation: PLADs=provincial-level administrative divisions.

areas of the program to ensure high routine coverage with two timely MCV doses, thereby reducing population susceptibility to measles.

Infants under eight months of age are generally susceptible to measles virus infection. In China, the first dose of the measles vaccine is administered at eight months, which is younger than the WHO-recommended age of nine months. Most infants acquire temporary passive protection from maternal measles antibodies transferred during gestation; however, maternal antibody levels significantly decrease by three months of age. This reduction results in minimal immunity in the months leading up to the first vaccine dose, placing these infants at risk of infection (*14*). Infants are indirectly protected when the incidence of measles is very low, but their susceptibility increases the risk of infection if measles circulates in the community. Therefore, maintaining high vaccination coverage to sustain population immunity is crucial for protecting children under eight months of age.

Recent surveillance data indicate that the majority of cases in children aged 8–23 months have a history of MCV immunization. Genotype analysis shows that the proportion of H1 genotype cases detected in 2018 was 89.8% (274/305), plummeting to 10.9% (30/275) in 2019 (*9*). No native H1 genotype cases were detected from 2020 onward, and all cases reported in 2021–2022 were associated with the vaccine-related A genotype (*5*,*15*). This suggests that many of these cases may be vaccine-associated rash illnesses rather than actual measles cases. This finding aligns with the absence of global spatial or temporal clustering of measles in recent years, given that the A genotype cannot transmit and cause epidemics. Therefore, it is crucial to promptly adjust and enhance the measles

monitoring program, improve the diagnosis of vaccine-associated rash illnesses, and align with ongoing measles elimination efforts.

Additionally, due to the highly contagious nature of measles, any epidemic worldwide poses a threat to China's efforts to eliminate the disease. Thus, China must prevent recurring domestic outbreaks and enhance monitoring of imported cases.

The study is subject to several limitations. First, as measles is a respiratory-transmitted disease, using provincial administrative divisions as spatial units for spatial clustering analyses might underestimate the clustering and fail to identify some localized outbreaks or epidemics. Second, some data used in this study are from the years immediately following the 2004 implementation of China's infectious disease reporting information management system. During the early stages of the system's development, there may have been information biases such as underreporting or misreporting.

In conclusion, measles surveillance data from 2005 to 2022 indicate that China has achieved moderate success in measles control, offering valuable insights for developing countries and bolstering global confidence in measles elimination. To sustain progress, it is crucial to maintain high two-dose MCV coverage among children, enhance prevention and control measures in high-risk populations and regions, improve the diagnosis of vaccine-associated rash illnesses, and continuously advance efforts toward measles elimination.

Conflicts of interest: No conflicts of interest.

Funding: Supported by the operation of the public health emergency response mechanism of the Chinese Center for Disease Control and Prevention (102393220020010000017).

doi: 10.46234/ccdcw2024.123

[#] Corresponding author: Zundong Yin, yinzd@chinacdc.cn.

[1] National Key Laboratory of Intelligent Tracking and Forecasting for Infectious Diseases, National Immunization Program, Chinese Center for Disease Control and Prevention, Beijing, China.

Submitted: January 23, 2024; Accepted: June 30, 2024

REFERENCES

1. Hope Simpson RE. Infectiousness of communicable diseases in the household (measles, chickenpox, and mumps). Lancet 1952;260(6734): 549 – 54. https://doi.org/10.1016/s0140-6736(52)91357-3.
2. WHO. Measles and rubella strategic framework: 2021-2030. 2021. https://measlesrubellapartnership.org/measles-rubella-strategic-framework-2021-2030/. [2023-11-20].
3. Ma C, Su QR, Hao LX, Wen N, Fan CX, Yang H, et al. Epidemiology of measles in China, 2017-2018. Chin J Vaccines Immun 2020;26(1): 5 – 8,41. https://doi.org/10.19914/j.cjvi.2020.01.002.
4. Ma C, Hao LX, Wen N, Fan CX, Yang H, Wang HQ, et al. Epidemiology of measles in China, 2019. Chin J Vaccines Immun 2020;26(5):493 – 7. https://doi.org/10.19914/j.cjvi.2020.05.002.
5. Liu QQ, Tang L, Wen N, Yang H, Wang XQ, Ma C, et al. Epidemiology of measles in China, 2020. Chin J Vaccines Immun 2022;28(2):135 – 9. https://doi.org/10.19914/j.CJVI.2022026.
6. Kim HJ, Fay MP, Feuer EJ, Midthune DN. Permutation tests for joinpoint regression with applications to cancer rates. Stat Med 2000;19 (3):335 – 51. https://doi.org/10.1002/(sici)1097-0258(20000215)19:3 <335::aid-sim336>3.0.co;2-z.
7. Maniragaba VN, Atuhaire LK, Rutayisire PC. Undernutrition among the children below five years of age in Uganda: a spatial analysis approach. BMC Public Health 2023;23(1):390. https://doi.org/10.1186/s12889-023-15214-9.
8. Shen JW, Pan JH, Wang Y, Zhao Q, Wang WB. Spatiotemporal distribution of measles in China, 2001-2016. Chin J Epidemiol 2021;42(4):608 – 12. https://doi.org/10.3760/cma.j.cn112338-20200317-00370.
9. Wang HL, Xu WB, Zhang Y. Progress of measles elimination in China. Natl Med J China 2023;103(26):2031-6. http://dx.doi.org/10.3760/cma.j.cn112137-20230308-00351. (In Chinese).
10. WHO. Measles reported cases and incidence. 2023. https://immunizationdata.who.int/global/wiise-detail-page/measles-reported-cases-and-incidence. [2023-11-17].
11. Minta AA, Ferrari M, Antoni S, Portnoy A, Sbarra A, Lambert B, et al. Progress toward measles elimination - worldwide, 2000-2022. MMWR Morb Mortal Wkly Rep 2023;72(46):1262 – 8. https://doi.org/10.15585/mmwr.mm7246a3.
12. Yu WZ, Li YQ, Wu J, Wang FZ, Wen N, Rodewald L, et al. Vaccination guidelines during and after the COVID-19 epidemic in China. China CDC Wkly 2020;2(34):661 – 5. https://doi.org/10.46234/ccdcw2020.169.
13. Guan J, Mahemutijiang, Fuerhati. Epidemiology of measles in Xinjiang, 2004-2010. Dis Surveill 2012;27(7):551 – 4. https://doi.org/10.3784/j.issn.1003-9961.2012.7.015.
14. Li SH, Wang JJ, Zhou J, Tang XH, Ling H. Establishment of a mathematical model for the analysis of anti-measles antibody reduction trend in children aged 1−8 months. Shanghai J Prev Med 2022;34(6): 568 – 70,576. https://doi.org/10.19428/j.cnki.sjpm.2022.21567.
15. Liu SY, Liu QQ, Li JH, Tang L, Wang XQ, Yang H, et al. Epidemiology of measles in China, 2021-2022. Chin J Vaccines Immun 2024;30(1):29 – 33. https://doi.org/10.19914/j.CJVI.2024006.

Methods and Applications

A New Integrated Interpolation Method for High Missing Unstable Disease Surveillance Data — 12 Urban Agglomerations, China, 2009–2020

Yuanhao Shi[1,2]; Yilan Liao[1,#]

ABSTRACT

Introduction: The prevalence of unstable and incomplete monitoring data significantly complicates syndromic analysis. Many data interpolation methods currently available demonstrate inadequate effectiveness in overcoming this issue.

Methods: To improve the accuracy of interpolation, we propose the integration of the SHapley Additive exPlanation model (SHAP) with the structural equation model (SEM), forming a combined SHAP-SEM approach. A case study is then performed to assess the enhanced performance of this novel model compared to traditional methods.

Results: The SHAP-SEM model was utilized to develop an interpolation model employing data from the Chinese respiratory syndrome surveillance database. We executed three distinct experiments to establish the model datasets, comprising a total of 100 replicates. The performance of the model was evaluated using the root mean square error (RMSE), correlation coefficient (r), and F-score. The findings demonstrate that the SHAP-SEM model consistently achieves superior accuracy in data interpolation, which is evident across different seasons and in overall performance.

Discussion: We conclude that the SHAP-SEM model demonstrates an exceptional capacity for accurately interpolating volatile and incomplete data. This capability is crucial for developing a comprehensive database that is essential for conducting risk assessments related to syndromes.

Syndrome surveillance is crucial for the rapid detection and alerting of infectious disease outbreaks. Nonetheless, it often encounters challenges including uneven distribution of monitoring sites, irregular reporting schedules, and incomplete data (*1*). These factors hinder the ability to accurately delineate disease distribution temporally and spatially, and to discern patterns and anomalies. Traditional spatio-temporal interpolation methods (*2*) are ill-suited for addressing the volatility and gaps in disease data, particularly when integrating significant influencing factors. Conversely, the structural equation model (SEM) facilitates analysis of complex data interactions to unearth underlying relationships among variables (*3*), thus enabling more precise interpolation. We suggest employing a SHapley Additive explanation (SHAP)-based SEM for the spatiotemporal interpolation of unstable and incomplete data.

METHODS

Shapley Additive ExPlanation Model with The Structural Equation Model (SHAP-SEM)

The SHAP model is utilized to evaluate multiple variables and their correlations with observed variables (*4*). It quantifies the marginal contribution of each variable to the model output, thereby demonstrating its influence on the overall model. This study aims to explore the relationship between meteorological variables and the virus positivity rate to identify the most impactful combination of these factors. Subsequently, the SEM is applied to discern the connections between the factors and observed variables (*3*), facilitating spatio-temporal interpolation. The SEM illustrates the network of relationships between meteorological variables and the virus, satisfying interpolation requirements based on the model fit. For further information on the SHAP-SEM model and additional classical interpolation methods, readers are referred to the Supplementary Material (available at https://weekly.chinacdc.cn/).

Model Assessment

In this study, the root mean square error (RMSE), correlation coefficient (r), and F-score were utilized to assess the accuracy of the SAHP-SEM and other comparative models.

RMSE measures the average difference between values predicted by a model and the actual values. It provides an estimation of how well the model can predict the target value (*5*).

The r quantifies the extent and direction of a linear relationship between two variables. Our research explores various methodologies, identifying that while Kriging interpolation displays a high determination coefficient, it unfortunately correlates poorly with the original dataset. This misalignment highlights its inability to accurately represent the underlying data trends. Consequently, due to the need for a precise reflection of these trends, we have chosen the r as our preferred metric.

The F-score is a composite metric that favors algorithms with higher sensitivity while penalizing those with higher specificity. It is derived from the precision and recall of the test. Here, precision refers to the number of true positive results divided by the total count of samples predicted as positive, inclusive of false positives. Recall, alternatively, is the number of true positives divided by the total number of samples that are correctly identified as positive (*6*). The F-score is formulated as follows (Equations 1–3):

$$Precision = \frac{TP}{TP + FP} \quad (1)$$

$$Recall = \frac{TP}{TP + FN} \quad (2)$$

$$F - score = \frac{2 \times Precision \times Recall}{Precision + Recall} \quad (3)$$

TP, FP, and FN denote true positives, false positives, and false negatives, respectively, across different classes. Precision quantifies the accuracy across various classes, recall indicates the detection rate, and the F-score provides a balanced measure of precision and recall.

Empirical Study

This study utilizes two primary data types: symptom data and meteorological data. Symptom data was derived from the China CDC's febrile respiratory syndrome surveillance, encompassing patient demographic profiles, clinical characteristics, and laboratory results obtained from 330 hospitals nationwide (Supplementary Figure S1, available at https://weekly.chinacdc.cn/). Meteorological data were sourced from the Meteorological Station Sharing Service System (https://data.cma.cn/). Selected meteorological parameters included atmospheric pressure, average relative humidity, mean temperature, maximum and minimum temperatures, and the range between the highest and lowest temperatures. Details on the variable utilization within the model are described in the Supplementary Material. For analysis, the SHAP-SEM model was applied to the China respiratory syndrome monitoring database to assess its effectiveness in disease interpolation. The period of study spanned from January 1, 2009 to January 4, 2020, with quarters serving as the smallest time unit. The study's scope of respiratory syndrome detection included various viruses: influenza virus (IFV), human respiratory syncytial virus (HRSV), human parainfluenza virus (HPIV), human adenovirus (HADV), human metapneumovirus (HMPV), and human coronavirus (HCOV).

All analyses were conducted using R software (version 4.1.2; R Foundation for Statistical Computing, Vienna, Austria). The "shapr" package facilitated the implementation of the SHAP process, and the "lavvn" package was utilized to construct the SEM model.

RESULTS

Supplementary Figure S2A (available at https://weekly.chinacdc.cn/) illustrates the seasonal distribution of six viruses across various regions. In major Chinese urban areas, the average absence rate of respiratory syndrome is 32.49%. Notably, the Central and Southern Liaoning and the Beibu Gulf urban agglomerations exhibit the highest absence rates, reaching 69.22%. In contrast, the Beijing-Tianjin-Hebei, Yangtze River Delta, and Pearl River Delta urban agglomerations show the lowest rates, all below 30%. To develop training and validation sets for our model, we randomly sampled various proportions of complete data. The model's accuracy is assessed using RMSE, r, and F-score metrics. Each virus demonstrates a distinct peak during the spring and winter festivals. IFV, HRSV, and HPIV are the predominant viruses among the general population. Geographically, IFV and HPIV are more prevalent in the north, whereas IFV and HRSV are more common in the south, as depicted in Supplementary Figure S2B. This regional variation persists, with HADV being more prevalent in the north. After data interpolation, the results shown in Figure 1 confirm consistent proportions of the three

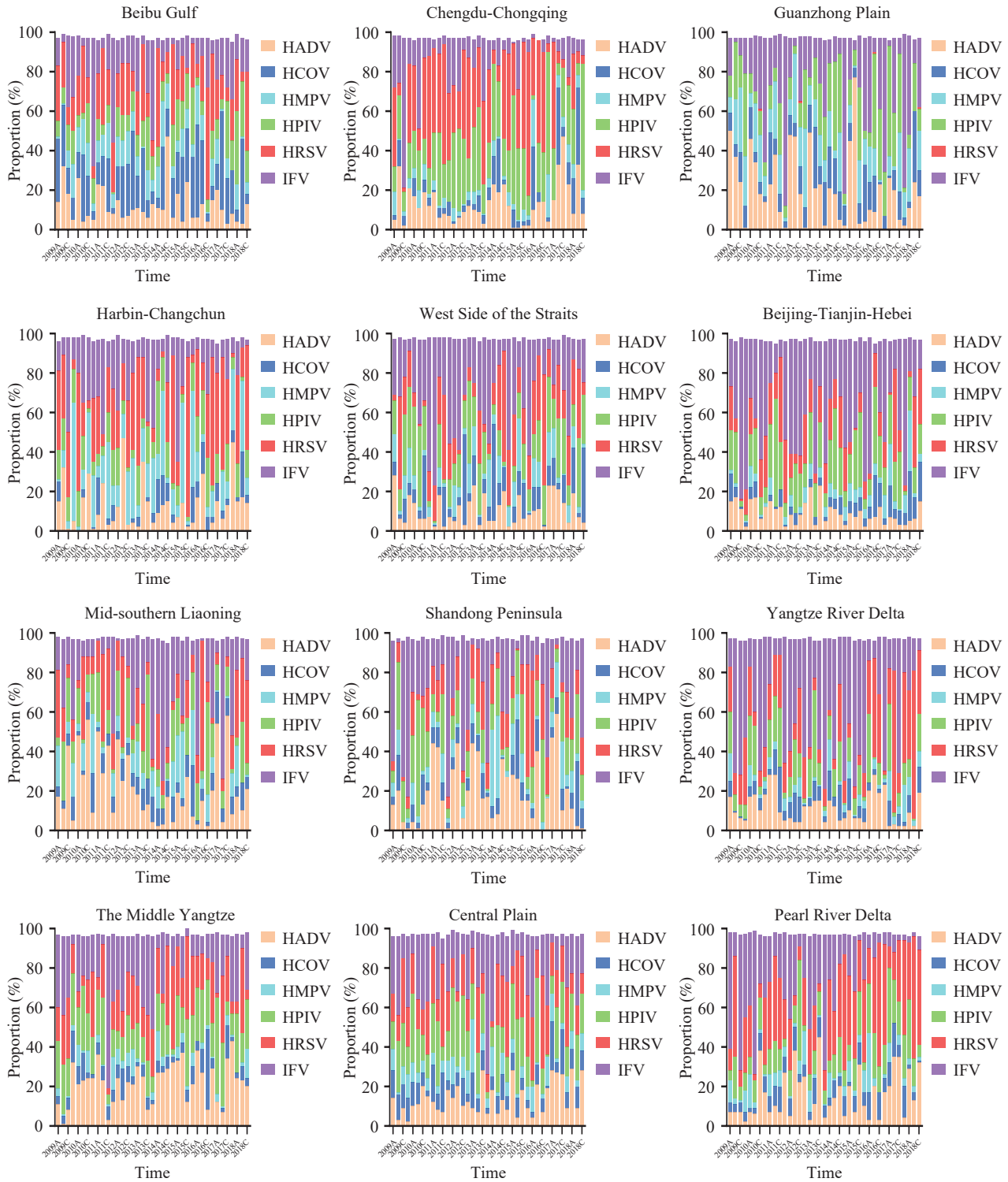

FIGURE 1. The virus structure spectrum of different urban agglomerations after interpolation.
Note: The letters "A" and "C" in the abscissa represent springand autumn quarters, respectively.
Abbreviation: HADV=human adenovirus; HCOV=human coronavirus; HMPV=human metapneumovirus; HPIV=human parainfluenza virus; HRSV=human syncytial virus; IFV=influenza virus.

primary viruses within the population. The north exhibits a higher prevalence of adenovirus as the primary virus, whereas the south displays a higher incidence of co-infections involving the IFV and syncytial virus.

The interpolation analysis delineates two distinct

TABLE 1. The average values of the three evaluation indicators under 100 repeated experiments for 5 models in each setting.

Methods	RMSE	r	F-score
Setting 1: Training=60%			
SHAP-SEM	5.813	0.710***	0.752
SEM	9.424	0.614**	0.651
Cokriging	8.273	0.429	0.634
Bayesian	10.174	0.494**	0.693
Sandwich	7.235	0.539***	0.621
Setting 2: Training=70%			
SHAP-SEM	5.157	0.734***	0.781
SEM	9.364	0.633**	0.684
Cokriging	8.047	0.457	0.634
Bayesian	9.154	0.518**	0.691
Sandwich	7.176	0.584***	0.633
Setting 3: Training=80%			
SHAP-SEM	5.081	0.767***	0.792
SEM	9.331	0.657*	0.708
Cokriging	7.524	0.461**	0.642
Bayesian	8.699	0.523**	0.701
Sandwich	6.926	0.601***	0.651

Abbreviation: RMSE=root-mean-square error; SHAP-SEM=SHapley Additive exPlanation model with the structural equation model; SEM=structural equation model.
* $P<0.05$;
** $P<0.01$;
*** $P<0.001$.

patterns in the dissemination of respiratory syndrome cases across China from 2009 to 2020. Supplementary Figure S2 categorizes Chinese urban agglomerations into three regions: the northern area, which includes the Central Plains; the central region, extending up to the middle reaches of the Yangtze River; and the combined southern and western areas, located beyond the middle reaches of the Yangtze River. In the first grouping, IFV predominated, followed by the parainfluenza virus, with adenoviruses appearing intermittently. The second group also had a predominance of IFV, with the syncytial virus as the second most prevalent, and adenoviruses appearing later in the sequence. In the third group, the syncytial virus was the most dominant, followed by the parainfluenza virus, with adenoviruses emerging in the first six months of the year. These findings have been validated in previous studies (*7–9*).

Table 1 presents the mean values of three evaluation metrics across 100 experimental replicates. The data demonstrates superior performance of the SEM integrated with the SHAP algorithm over traditional methods, notably in comparison to the conventional SEM, across all assessed metrics. This indicates enhanced and more consistent interpolation accuracy with the SHAP-SEM approach. Additionally, enlarging the training set size contributes to improved interpolation precision. Compared to the conventional SEM, the SHAP-SEM model excels in spatial distribution accuracy and primary virus classification accuracy. Overall, the SHAP-SEM model achieves robust performance across all indices. Kriging shows the lowest RMSE, but exhibits a decreased r value, whereas the Bayesian approach maintains a relatively high F-score.

Table 2 presents the mean values of evaluation metrics across various simulation settings for different quarters. The findings reveal that accuracy peaks during the winter and dips to its lowest in the autumn. The SHAP-SEM model exhibits superior performance

TABLE 2. Average values of the three evaluation indicators in different seasons under 100 repeated experiments for 5 models in each setting.

Quarters	Method	RMSE	r	F-score
Spring	SHAP-SEM	4.214	0.781***	0.811
	SEM	5.019	0.722**	0.736
	Cokriging	5.105	0.581*	0.662
	Bayesian	6.428	0.614**	0.705
	Sandwich	6.832	0.637**	0.651
Summer	SHAP-SEM	6.194	0.703**	0.710
	SEM	10.521	0.641**	0.682
	Cokriging	7.113	0.519	0.627
	Bayesian	9.245	0.588*	0.690
	Sandwich	8.194	0.572*	0.638
Autumn	SHAP-SEM	7.237	0.651**	0.631
	SEM	9.144	0.601*	0.614
	Cokriging	6.184	0.467	0.596
	Bayesian	7.965	0.501	0.587
	Sandwich	8.229	0.523*	0.577
Winter	SHAP-SEM	4.057	0.722***	0.753
	SEM	6.124	0.671***	0.707
	Cokriging	5.016	0.514*	0.636
	Bayesian	7.255	0.635**	0.641
	Sandwich	5.417	0.642**	0.639

Abbreviation: MSE=mean-square error; RMSE=root-mean-square error; SHAP-SEM=SHapley Additive exPlanation model with the structural equation model; SEM=Structural equation model.
* $P<0.05$;
** $P<0.01$;
*** $P<0.001$.

in the winter, markedly enhancing accuracy relative to competing models. Conversely, in the autumn, the sandwich interpolation method surpasses the SHAP-SEM model in terms of accuracy enhancement.

DISCUSSION

Missing data frequently complicates syndromic surveillance, obstructing the analysis of disease patterns and trends, thereby impeding efforts in disease prevention and control. Developing methods for data interpolation in environments characterized by unstable monitoring and significant data gaps presents a formidable research challenge. Conventional interpolation techniques are often inadequate in contexts involving complex interactions between diseases and their determinants. These methods generally underperform in addressing missing values within sparse datasets.

This study employed interpolation techniques to estimate the prevalence of primary viruses associated with seasonal respiratory syndrome across 13 major urban areas in China between 2010 and 2018, accounting for sparse data and missing values. The accuracy of these estimates was assessed using RMSE, r, and F-score. The results indicate that this method surpasses other approaches in enhancing the accuracy of data on primary respiratory syndrome viruses, achieving significant improvements in overall and seasonal accuracy.

Most spatiotemporal interpolation models for diseases incorporate both spatiotemporal autocorrelation and differentiation. The Co-kriging method (*10*) is a geostatistical technique leveraging correlations between various variables across different sites for spatial interpolation and prediction. However,

employing Co-kriging to estimate missing data introduces increased uncertainty because these estimations depend heavily on the availability of complete datasets and on the spatial correlation among variables. A lack of data in a dataset can undermine spatial autocorrelation, rendering predictions unreliable. Bayesian hierarchical models (*11*) attempt to manage missing data under the assumption of random data loss. If the missing data mechanism is misrepresented within the model, however, parameter estimations might be biased. Conventionally, it is assumed that data loss is random; however, overlooking the specific missing data mechanism can lead to biases in the estimated parameters due to improper data handling. The sandwich approach (*12*) further complicates the issue by treating missing and observed data as independent, disregarding any patterns or correlations in the data removal process. This can result in incorrect standard errors and inferences, particularly when the data deletion mechanisms are informative or directly linked to the variables of interest. Additionally, the complex dynamics of disease occurrence, infection, and transmission intersect variably with different factors. To enhance spatiotemporal interpolation accuracy, advanced techniques like deep learning, including random forest models (*13*) and regressive neural networks (*14*), have been utilized. Despite their effectiveness, these models are often complex and do not sufficiently address the multifaceted nature of disease prevention. This study proposes the integration of SEM with SHAP to discern crucial features and their interrelationships, thus tackling issues related to unstable and fragmented data in health monitoring. By resolving these issues and synthesizing them within our research, we can derive precise insights about syndromes, affected regions, and causal factors. This approach promises to yield scientifically based recommendations for efficacious local prevention and control strategies.

However, this study is subject to some limitations. The SHAP-SEM model necessitates a large sample size, which may not always be feasible with incomplete syndrome surveillance data. Additionally, it is crucial to recognize that viral activity is influenced by a range of risk factors. Future endeavors to integrate incomplete syndrome monitoring data with the SHAP-SEM model should include more factors. It is also important to note that the scalability of SHAP-SEM models may be compromised when handling large datasets. As the size of the dataset expands, the computational and memory demands escalate, potentially leading to extended processing times and heightened complexity.

In further studies, comprehensive descriptions and analyses of the syndrome's spatial and temporal distribution can be achieved through interpolation methods. Additionally, examining variations in viral activity and seasonal trends across different regions is possible. Building on this knowledge, identifying specific risk groups and areas becomes feasible, providing essential data to support targeted, time-sensitive, and location-specific prevention and control strategies.

Conflicts of interest: No conflicts of interest.

Funding: Supported by the Foundation of China (grant number 42171419) and National Science and Technology Major Project of China (grant number 2018ZX10713001).

doi: 10.46234/ccdcw2024.124

[#] Corresponding author: Yilan Liao, liaoyl@lreis.ac.cn.

[1] The State Key Laboratory of Resources and Environmental Information System, Institute of Geographic Sciences and Natural Resources Research, Chinese Academy of Sciences, Beijing, China; [2] University of Chinese Academy of Science, Beijing, China.

Submitted: May 06, 2024; Accepted: July 01, 2024

REFERENCES

1. Jia P, Yang SJ. China needs a national intelligent syndromic surveillance system. Nat Med 2020;26(7):990. https://doi.org/10.1038/s41591-020-0921-5.
2. Koch T. Disease mapping and innovation: a history from wood-block prints to Web 3. 0. Patterns 2022;3(6):100507. https://doi.org/10.1016/j.patter.2022.100507.
3. Lee KY, Li LX. Functional structural equation model. J Roy Stat Soc Ser B Stat Methodol 2022;84(2):600 – 29. https://doi.org/10.1111/rssb.12471.
4. Liu YC, Liu ZH, Luo X, Zhao HJT. Diagnosis of Parkinson's disease based on SHAP value feature selection. Biocybern Biomed Eng 2022;42(3):856 – 69. https://doi.org/10.1016/j.bbe.2022.06.007.
5. Willmott CJ, Matsuura K. Advantages of the mean absolute error (MAE) over the root mean square error (RMSE) in assessing average model performance. Climate Res 2005;30(1):79 – 82. https://doi.org/10.3354/cr030079.
6. Zhang WG, He YW, Wang LQ, Liu SL, Meng XY. Landslide susceptibility mapping using random forest and extreme gradient boosting: a case study of Fengjie, Chongqing. Geol J 2023;58(6):2372 – 87. https://doi.org/10.1002/gj.4683.
7. Li ZJ, Zhang HY, Ren LL, Lu QB, Ren X, Zhang CH, et al. Etiological and epidemiological features of acute respiratory infections in China. Nat Commun 2021;12(1):5026. https://doi.org/10.1038/s41467-021-25120-6.
8. Wang JL, Chen T, Deng LL, Han YJ, Wang DY, Wang LP, et al. Epidemiological characteristics of imported respiratory infectious diseases in China, 2014−2018. Infect Dis Poverty 2022;11(1):22. https:

//doi.org/10.1186/s40249-022-00944-6.
9. Zhao YJ, Lu RJ, Shen J, Xie ZD, Liu GS, Tan WJ. Comparison of viral and epidemiological profiles of hospitalized children with severe acute respiratory infection in Beijing and Shanghai, China. BMC Infect Dis 2019;19(1):729. https://doi.org/10.1186/s12879-019-4385-5.
10. Xiao MY, Zhang GH, Breitkopf P, Villon P, Zhang WH. Extended Co-Kriging interpolation method based on multi-fidelity data. Appl Math Comput 2018;323:120 – 31. https://doi.org/10.1016/j.amc.2017.10.055.
11. Miller PC, Ren MD, Schlame M, Toth MJ, Phoon CKL. A bayesian analysis to determine the prevalence of barth syndrome in the pediatric population. J Pediatr 2020;217:139 – 44. https://doi.org/10.1016/j.jpeds.2019.09.074.
12. Wang JF, Haining R, Cao ZD. Sample surveying to estimate the mean of a heterogeneous surface: reducing the error variance through zoning. Int J Geogr Inf Sci 2010;24(4):523 – 43. https://doi.org/10.1080/13658810902873512.
13. Mariano C, Mónica B. A random forest-based algorithm for data-intensive spatial interpolation in crop yield mapping. Comput Electron Agric 2021;184:106094. https://doi.org/10.1016/j.compag.2021.106094.
14. Abdelaziz M, Wang TF, Elazab A. Alzheimer's disease diagnosis framework from incomplete multimodal data using convolutional neural networks. J Biomed Inform 2021;121:103863. https://doi.org/10.1016/j.jbi.2021.103863.

SUPPLEMENTARY MATERIAL

SHAP-SEM Model

The fundamental concept of SHapley Additive exPlanation model (SHAP) is to facilitate both global and local interpretations through the evaluation of the marginal contributions of variable features. This approach assists users in comprehending the relative importance of each feature, thereby enabling effective variable filtering.

The SHAP model utilizes pre-processed data for each variable alongside the target variable. The Shapley values of individual variables are then calculated to assess their relationships with the target variable (Equation 4).

$$\hat{\varphi}_j = \frac{1}{M}\sum_{m=1}^{M}\left(f\left(x_{+j}^{m}\right) - f\left(x_{-j}^{m}\right)\right) \tag{4}$$

Where $\hat{\varphi}_j$ represents the Shapley value of the feature of the variable, j, M represents the total number of instances, f represents the kernel function, x_{+j}^{m} represents the entire instance containing the feature of the variable, and j, and x_{-j}^{m} represents the entire instance without the feature of the variable j.

In this study, we utilized quarterly non-normalized positivity rates along with meteorological variables from various urban agglomerations to construct SHAP models. Employing the edge effect approach, we calculated the significance of various variables on respiratory viruses and their inter-variable interactions. The impact of different combinations of influencing variables on respiratory viruses is presented in Equation 5.

$$\hat{v}(S) = \frac{1}{M}\sum_{k=1}^{M}\left(f\left(x_S^{(i)} \cup x_C^{(k)}\right) - f\left(x^{(k)}\right)\right) \tag{5}$$

$\hat{v}$ represents changes in the respiratory virus in the S variable combination; S is a combination of different variables; x_S and x_C represent all instances that contain S combinations and instances that do not contain S combinations.

Structural equation models (SEMs) elucidate variations within variables and the covariation among them while investigating the relationships between observed and latent variables. SEMs typically comprise two components: the measurement model, which analyzes the relationships between latent variables and their indicators, and the path model, which explores the relationships among the variables themselves.

In this study, the meteorological variables from the SHAP model were used as input variables in the SEM model, with the non-normalized positivity rate of respiratory viruses serving as the observed variables. The framework of the bipartite SEM model was structured accordingly (Equations 6–7).

$$Y_i = \lambda_i \eta + \delta_i \tag{6}$$

$$\eta_i = \sum_{\substack{j=1 \\ j \neq i}}^{J} b_{ij}\eta_j + \epsilon_i \tag{7}$$

Where Y_i is the value of the *ith* observed variable; λ_i represents the factor load between the observed variable and the variable under the value of the *ith* observed variable; η represents the variable that passes the significance test of Shapley value; δ and ϵ represent the error of the measurement model and the path model respectively, and b represents the path coefficient between the variable i and variable j, which means the interaction between the two variables.

Cokriging Method

Cokriging, a geostatistical method initially developed for mining applications, is extensively used in soil science. The primary instrument in geostatistics is the semivariogram, which quantifies the spatial dependence among adjacent observations. The semivariogram, $\gamma(h)$, can be defined as half the variance of the difference in attribute values at all pairs of points separated by h as Equation 8 (*1*).

$$\gamma(h) = \frac{1}{2N(h)}\sum_{i=1}^{N(h)}\left[Z(x_i) - Z(x_i + h)\right]^2 \tag{8}$$

where $Z(x)$ indicates the magnitude of variables, and $N(h)$ is the total number of pairs of attributes that are separated by a distance h.

SUPPLEMENTARY TABLE S1. Geographical distribution of 12 urban agglomerations in China.

UAs	Cities/Municipalities
Central Plain UA	Handan, Xintai, Changzhi, Jincheng, Yuncheng, Bengbu, Fuyang, Suzhou, Bozhou, Liaocheng, Heze, Zhengzhou, Kaifeng, Luoyang, Pingdingshan, Anyang, Hebi, Xinxiang, Jiaozuo, Puyang, Xuchang, Leihe, Sanmenxia, Nanyang, Shangqiu, Xinyang, Zhoukou, Zhumadian
Beijing-Tianjin-Hebei UA	Beijing, Tianjin, Shijiazhuang, Tangshan, Qinhuangdao, Baoding, Zhangjiakou, Chengde, Langfang, Cangzhou
Guanzhong Plain UA	Xi'an, Tongchuan, Baoji, Xianyang, Weinan, Shangluo, Tianshui
Beibu Gulf UA	Zhanjiang, Maoming, Yangjiang, Nanning, Beihai, Fangchenggang, Qinzhou, Yulin, Chongzuo, Haikou
Harbin-Changchun UA	Changchun, Jilin, Siping, Liaoyuan, Songyuan, Yanbian, Harbin, Qiqihaer, Daqin, Mudanjiang, Suihua
Shandong Peninsula UA	Jinan, Qindao, Zibo, Dongying, Yantai, Weifang, Weihai, Rizhao
Chendu-Chongqing UA	Chongqing, Chendu, Zigong, Luzhou, Deyang, Mianyang, Suining, Neijiang, Leshan, Nanchong, Meishan, Yibing, Guangan, Dazhou, Yaan, Ziyang
West Side of Straits UA	Wenzhou, Quzhou, Lishui, Fuzhou, Xiamen, Putian, Sanming, Quanzhou, Zhangzhou, Nanping, Longyan, Ningde, Ganzhou, Shantou, Meizhou, Chaozhou, Jieyang
Pearl River Delta UA	Guangzhou, Shenzhen, Zhuhai, Foshan, Jiangmen, Zhaoqin, Huizhou, Shanwei, Heyuan, Qinyuan, Dongwan, Zhongshan, Yunfu
Mid-southern Liaoning UA	ShenYang, Dalian, Anshan, Fushun, BenXi, Dandong, Yinkou, Liaoyang, Panjin
Yangtze River Delta UA	Shanghai, Nanjing, Wuxi, Changzhou, Suzhou, Nantong, Yancheng, Yangzhou, Zhenjiang, Taizhou, Ningbo, Jiaxin, Huzhou, Shaoxin, Jinhua, Zhoushan, Taizhou, Hefei, Wuhu, Maanshan, Tonglin, Anqin, Chuzhou, Chizhou, Xuancheng
The Middle Yangtze UA	Nanchang, Jingdezhen, Pingxiang, Jiujiang, Xinyu, Yintan, Jian, Yichun, Fuzhou, Shangrao, Wuhan, Huangshi, Yichang, Ezhou, Jinmen, Xiaogan, Jinzhou, HUanggang, Xianning, Changsha, Zhuzhou, Xiangtan, Hengyang, Yueyang, Chnagde, Yiyang, Loudi

Abbreviation: UA=urban agglomeration.

Bayesian Hierarchical Model

The framework of Bayesian hierarchical modeling consists of a structured approach to model building where unobserved quantities are categorized into distinct levels with clear, scientifically interpretable functions and probabilistic connections that reflect the intrinsic characteristics of the data. This methodology has been successfully applied in the analysis of complex epidemiological, biomedical, environmental, and various other types of data (*2*).

Spatial Sandwich Model

The concept of sandwich space interpolation is based on dual-layer stratified statistics. This process constructs an information transfer function across three hierarchical levels: the object layer, the zoning layer, and the reporting layer. Initially, attributes at the object layer are categorized or divided into different zones (zoning layer), followed by stratified sampling within these zones. Specifically, at least two sample points per category are chosen to calculate the mean and variance for each group. Subsequently, these statistical measures are transferred to the reporting layer through overlaying it with the zoning layer. This allows for the compilation of mean and variance for each reporting unit, thereby facilitating the generation of a spatial interpolation map and its corresponding error distribution map (*3*).

Data and Descriptive Analysis

Meteorological data were gathered from 756 ground-based weather stations across China, accessed via the meteorological station sharing service system (https://data.cma.cn/). The selected meteorological variables for this study include atmospheric pressure, average relative humidity, average temperature, average maximum temperature, average minimum temperature, and the range between the highest and lowest temperatures. Daily meteorological data were consolidated into monthly averages. For other study areas, data were estimated using Kriging interpolation, and averages of urban meteorological parameters within urban conglomerates were calculated to derive the aggregate meteorological data for urban agglomerations.

The initial surveillance data indicated a total of 39,760 pneumonia cases, representing 19.63% of the 202,539 samples analyzed. Among the total study population, 76,450 were children under five years of age, constituting 37.75% of the total. Of these, 16,867 cases of pneumonia were children, making up 42.42% of all pneumonia cases. According to Supplementary Table S2, IFV and HRSV were the largest viruses detected in each season, accounting

SUPPLEMENTARY TABLE S2. Number of detections for each virus by season.

Virus	Spring	Summer	Autumn	Winter	Sum
IFV	3,372	3,141	3,397	9,399	19,309
HRSV	1,927	1,020	2,230	4,094	9,271
HPIV	2,002	1,997	1,647	1,301	6,947
HADV	1,509	1,462	1,238	1,589	5,798
HMPV	869	257	269	748	2,143
HCOV	760	850	636	668	2,914
Sum	10,439	8,727	9,417	17,799	46,382

Abbreviation: HADV=human adenovirus; HCOV=human coronavirus; HMPV=human metapneumovirus; HPIV=human parainfluenza virus; HRSV=human syncytial virus; IFV=influenza virus.

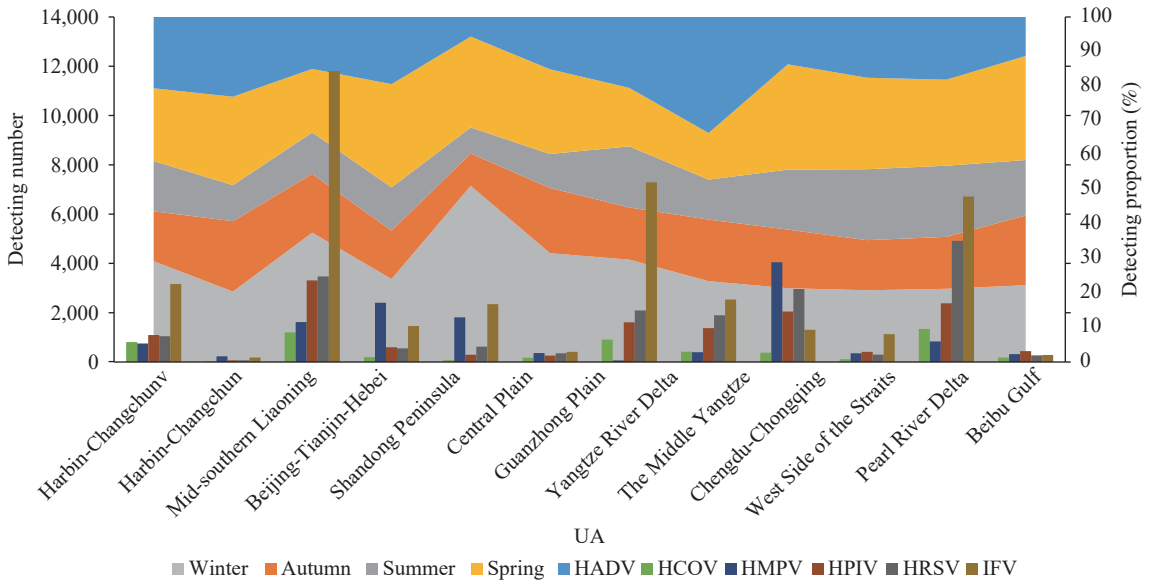

SUPPLEMENTARY FIGURE S1. Distribution of raw data and quarterly distribution by UAs.
Abbreviation: UA=urban agglomeration; HADV=human adenovirus; HCOV=human coronavirus; HMPV=human metapneumovirus; HPIV=human parainfluenza virus; HRSV=human syncytial virus; IFV=influenza virus.

for 41.63% and 19.99% of the total samples. IFV in winter accounted for the largest proportion of all viruses detected in all seasons with a percentage of 52.81% and 20.26% of the total annual samples.

Supplementary Figure S1 presents the original monitoring data for each urban agglomeration, segmented by quarter. The Beijing-Tianjin-Hebei, Pearl River Delta, and Yangtze River Delta urban agglomerations lead in monitoring volume. In contrast, the Mid-southern Liaoning and Guanzhong Plain urban agglomerations recorded the lowest sample numbers. Notably, the proportion of HMPV in the Shandong Peninsula, Central Plains, and Chengdu-Chongqing urban agglomerations is significantly higher than in others, while the prevalence of HADV and IFV is notably lower.

Model Setting

Our simulation study investigates six principal configurations by segmenting the quarter and urban agglomerations with monitoring data into separate training and validation sets. These configurations are subsequently applied to SHAP-SEM and other conventional interpolation models.

Setting 1: Training=60%, Valid=40%;

Setting 2: Training=70%, Valid=30%;

Setting 3: Training=80%, Valid=20%;

Utilization of Variables

The Kriging interpolation method employs the covariance function of the virus under the assumption of second-order stationarity. Bayesian interpolation is based on Bayesian probability theory. Sandwich interpolation utilizes stratified sampling and considers spatial variations for interpolation. SEM is used to model and interpolate the network diagram of structural relationships, where meteorological elements and the virus are depicted as nodes, and their interconnections as edges. The SHAP-SEM approach quantifies the marginal effects of meteorological variables on the virus and identifies significant contributors for inclusion in further SEM analysis.

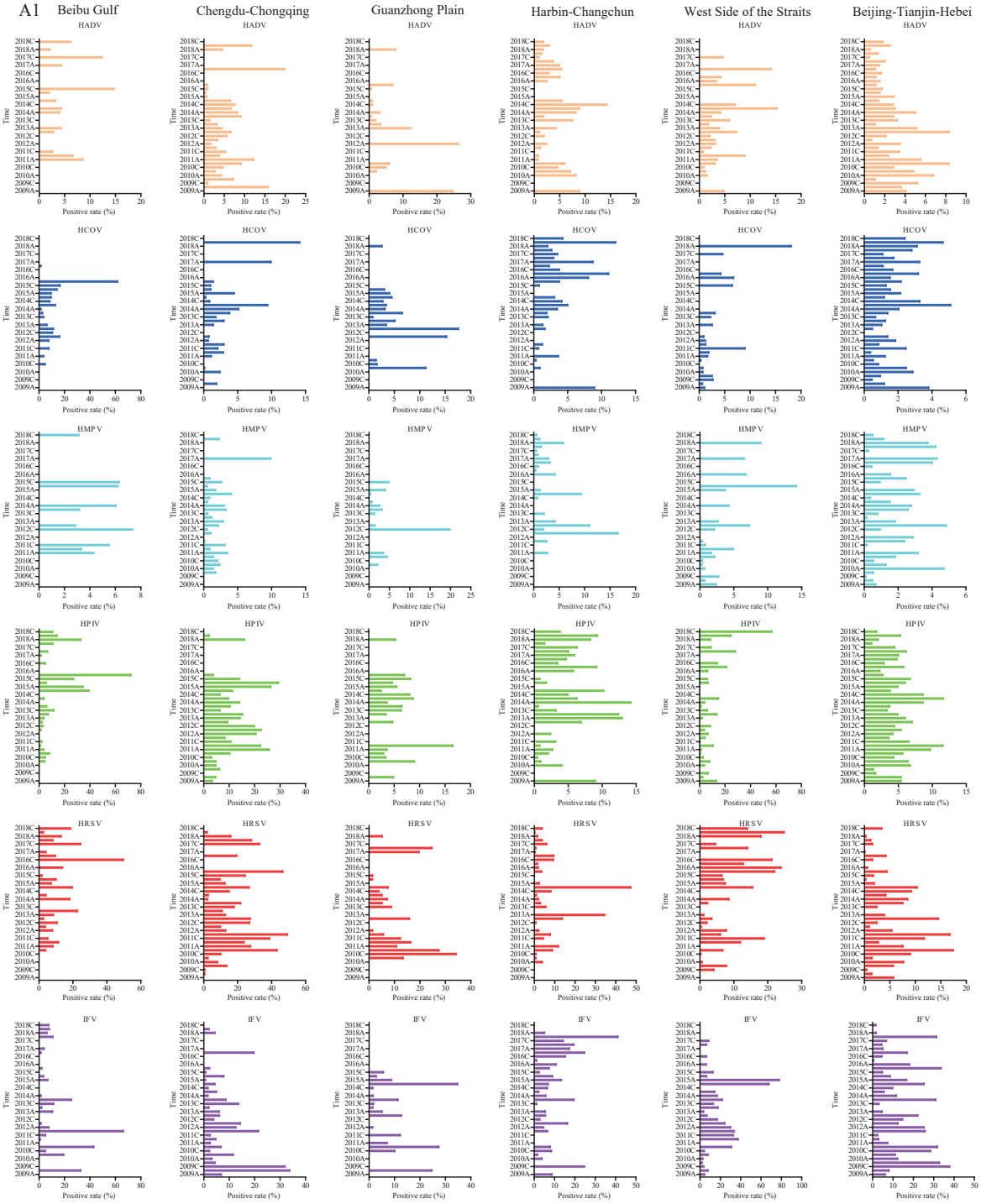

A2 Mid-southern Liaoning | Shandong Peninsula | Yangtze River Delta | the Middle Yangtze | Central Plain | Pearl River Delta

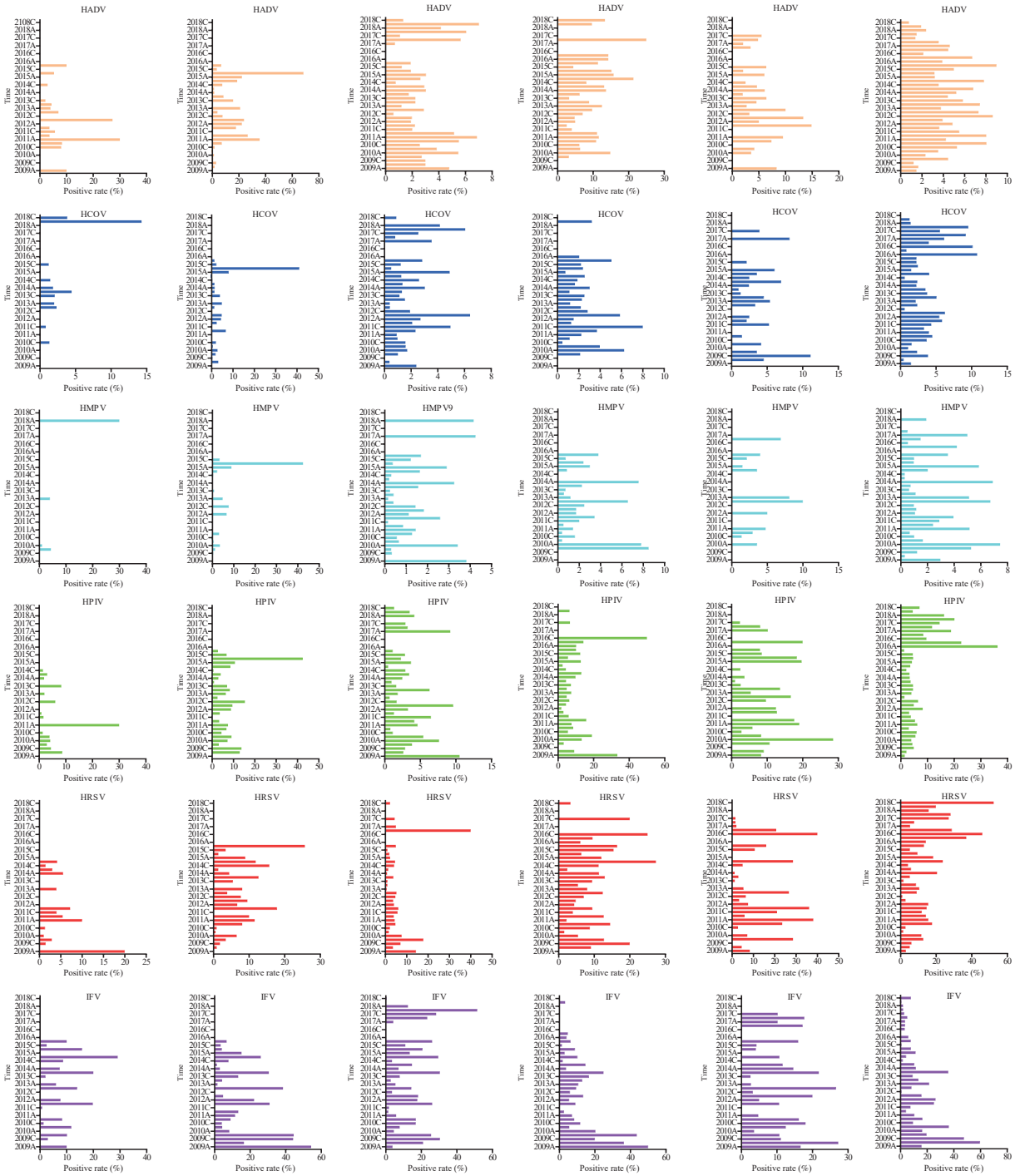

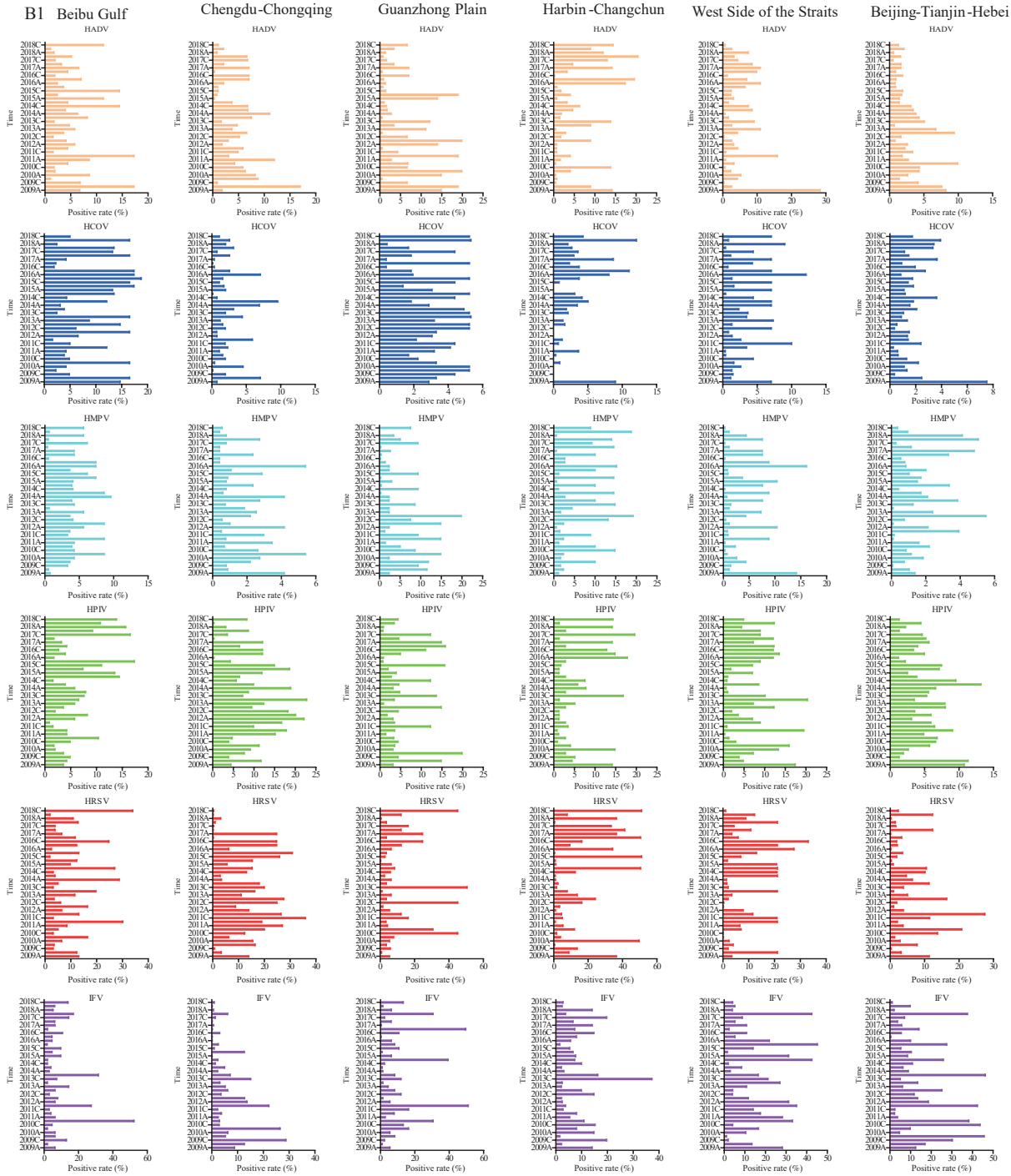
B1 Beibu Gulf
Chengdu-Chongqing
Guanzhong Plain
Harbin-Changchun
West Side of the Straits
Beijing-Tianjin-Hebei
HADV
HCOV
HMPV
HPIV
HRSV
IFV
Time
Positive rate (%)

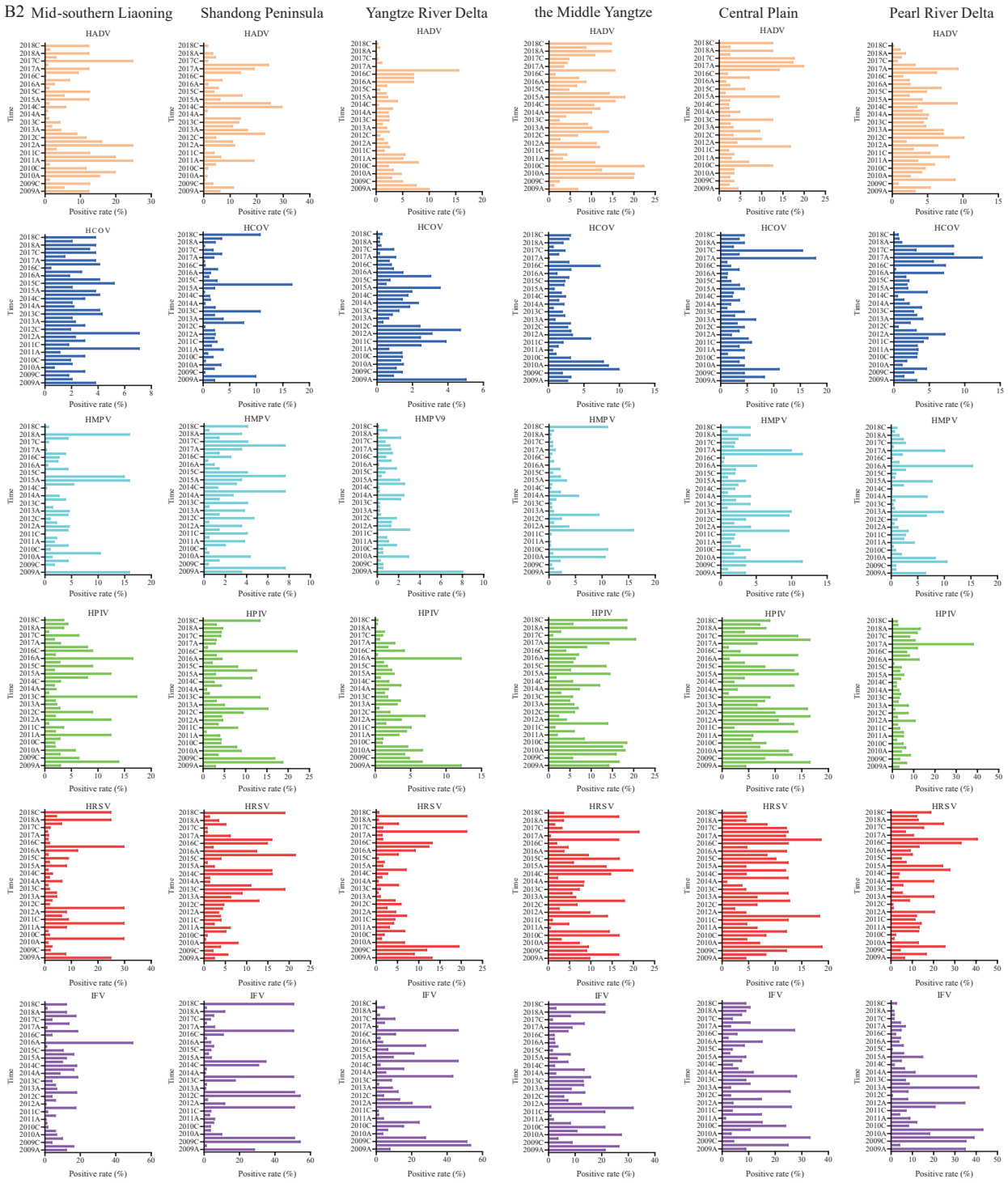

SUPPLEMENTARY FIGURE S2. Virus positive rates in different urban agglomerations. (A) Before interpolation; (B) After interpolation.

Note: A1 and B1 include six UAs: Beibu Gulf, Chengdu-Chonqing, Guanzhong Plain, Harbin-Changchun, West side of the Straits, and Beijing-Tianjing-Hebei. A2 and B2 include other six UAs: Mid-southern Liaoning, Shandong Peninsula, Yangtze River Delta, the Middle Yangtze, Central Plain, and Pear River Delta. The letters “A” and “C” in the ordinate represent spring and autumn quarters, respectively.

Abbreviation: HADV=human adenovirus; HCOV=human coronavirus; HMPV=human metapneumovirus; HPIV=human parainfluenza virus; HRSV=human syncytial virus; IFV=influenza virus.

REFERENCES

1. Ahmadi SH, Sedghamiz A. Application and evaluation of kriging and cokriging methods on groundwater depth mapping. Environ Monit Assess 2008;138(1-3):357 – 68. https://doi.org/10.1007/s10661-007-9803-2.
2. Richardson S, Best N. Bayesian hierarchical models in ecological studies of health–environment effects. Environmetrics 2003;14(2):129 – 47. https://doi.org/10.1002/env.571.
3. Wang JF, Haining R, Cao ZD. Sample surveying to estimate the mean of a heterogeneous surface: reducing the error variance through zoning. Int J Geogr Inf Sci 2010;24(4):523 – 43. https://doi.org/10.1080/13658810902873512.

Outbreak Reports

A Case of Brucellosis Concomitant with Severe Fever with Thrombocytopenia Syndrome — Weifang City, Shandong Province, China, 2023

Qingqing Xu[1,&]; Cuiping Wu[2,&]; Hui Liu[3,&]; Chao Geng[4]; Jinhui Zhang[1]; Dongri Piao[1]; Hongyan Zhao[1]; Yu Fan[1]; Guozhong Tian[1]; Hai Jiang[1,#]

Summary

What is already known about this topic?

Brucellosis and severe fever with thrombocytopenia syndrome (SFTS) are neglected zoonoses, attributable respectively to *Brucella* and the SFTS virus (SFTSV). While the incidence of these diseases has been rising, instances of co-infection remain uncommon.

What is added by this report?

This represents the first documented case of a rare coinfection involving *Brucella* and SFTSV. We carried out an epidemiological analysis of patients diagnosed with brucellosis and those with SFTS at Yidu Central Hospital of Weifang. Our findings demonstrate a temporal and spatial overlap among the affected individuals.

What are the implications for public health practice?

Our findings suggest that co-infections arising from the spatiotemporal overlap of *Brucella* and SFTSV are plausible, necessitating heightened awareness and enhanced diagnostic measures.

On July 26, 2023, a patient exhibiting an unexplained fever was admitted to Yidu Central Hospital of Weifang. The diagnosis of brucellosis was confirmed based on clinical symptoms, epidemiological history, the *Brucella* Rose Bengal test, and the serum agglutination test. Despite receiving treatment, the patient's platelet counts continued to decline. Subsequent testing using reverse transcription-polymerase chain reaction (RT-PCR) led to an additional diagnosis of severe fever with thrombocytopenia syndrome (SFTS), indicating a co-infection with *Brucella* and SFTS virus (SFTSV). To our knowledge, this is the first reported case of simultaneous brucellosis and SFTS, underscoring the necessity of integrated prevention strategies for multiple zoonotic diseases. Medical practitioners should maintain vigilance for local endemic diseases and consider the potential for concurrent infections to prevent treatment delays.

INVESTIGATION AND RESULTS

A 52-year-old female was referred to Yidu Central Hospital of Weifang presenting with fever, generalized muscle and joint pain, chills, severe fatigue, and diminished appetite. The patient, a farmer resident in Changle County, Weifang City, Shandong Province, reported extensive contact with sheep and other livestock.

On July 17, 2023, the patient developed a fever, registering a temperature of 38.9 ℃. Despite receiving treatment at a local hospital for three days, her temperature continued to fluctuate. She reported experiencing a worsening of symptoms.

On July 26, 2023, a patient presented at Yidu Central Hospital of Weifang for evaluation; initial blood tests conducted prior to admission indicated leukopenia. She was assessed in the outpatient clinic with a primary diagnosis of unexplained fever. The findings from the physical examination at the time of admission included a temperature of 38.5 ℃, a respiratory rate of 22 breaths per minute, a pulse rate of 86 beats per minute, and a blood pressure of 123/78 mmHg. The patient was alert but appeared lethargic and was minimally responsive. Examination revealed slight yellowing of the skin and sclera, with no accompanying rash. A tender lymph node approximately the size of a peanut was palpable in the right groin. Examination of the heart and lungs did not disclose any significant abnormalities. Laboratory tests showed decreased leukocyte and platelet counts, while elevations were noted in ferritin, procalcitonin, C-reactive protein, and interleukin-6 levels (Table 1). The Rose Bengal test for *Brucella* and the serum agglutination test at a titer of 1∶200 were both

TABLE 1. Laboratory test results of a case with brucellosis and SFTS in Yidu Central Hospital of Weifang in 2023.

Test items	Days after onset (date)					Normal range
	8 (7.25)	9 (7.26)	10 (7.27)	15 (8.1)	17 (8.3)	
White blood cell count (10^9/L)	2.34	2.67	3.78	7.69	6.07	3.5–9.5
Neutrophil percentage (%)	46.3	48.4	53.6	–	–	40–75
Red blood cell (10^{12}/L)	4.56	4.15	4.26	–	–	3.8–5.1
Hemoglobin (g/L)	119	124	109	–	–	115–150
Platelet (10^9/L)	100	93	80	82	108	125–350
Ferritin (ng/mL)	–	929	–	–	300	15–200
Procalcitonin (ng/mL)	–	0.253	–	–	0.031	<0.15
C-reactive protein (mg/mL)	–	68	–	–	21	0–10
Interleukin-6 (pg/mL)	–	149.3	–	–	18.34	<7
Alanine aminotransferase (U/L)	–	–	484	92	42	7–40
Aspartate aminotransferase (U/L)	–	–	839	44	33	13–35
Total bile acids (μmol/L)	–	–	92.9	2.3	–	0.1–10.0
Total protein (g/L)	–	–	53.9	64.6	–	55–80
Albumin (g/L)	–	–	33.7	34.6	–	35–55
Total bilirubin (μmol/L)	–	–	44.8	13.6	21	1.71–21.00
Direct bilirubin (μmol/L)	–	–	39.9	9.1	13	0–6.8
Alkaline phosphatase (U/L)	–	–	407	282	57	35–100
Lactate dehydrogenase (U/L)	–	–	690	329	248	313–618
Creatine kinase (U/L)	–	–	1261	498	65	40–200
Creatine kinase isoenzyme (U/L)	–	–	342	201	23	<5.0
Sodium (mmol/L)	–	–	126	142	–	135–145

Note: "–" indicates that this test was not performed on that day.
Abbreviation: SFTS=severe fever with thrombocytopenia syndrome.

positive, confirming an infection with *Brucella*. Antibiotic therapy was subsequently initiated.

On July 27, 2023, the patient exhibited a significant drop in platelet count to 80×10^9/L. Although renal function, blood glucose, and lipid levels remained within normal limits, elevated levels were noted in several liver function markers — including alanine aminotransferase, aspartate aminotransferase, total bile acids, alkaline phosphatase, lactate dehydrogenase — as well as in creatine kinase and its isoenzymes (Table 1). Electrolyte concentrations were overall stable, with the exception of a decreased sodium level (Table 1). Imaging using superficial lymph node B-ultrasound identified a lymph node measuring 2cm by 1cm with distinct borders in the right groin. Further laboratory analysis using RT-PCR detected SFTSV nucleic acids in the serum at a concentration of 5.52×10^4 copies/mL. Based on these clinical findings and laboratory data, the patient was diagnosed with SFTS and subsequently received symptomatic treatment.

On July 28, 2023, the patient's blood culture tested positive for *Brucella melitensis* biovar 3, confirming an infection with brucellosis.

On August 1, 2023, the patient's condition and laboratory indicators stabilized. By August 3, 2023, the patient was discharged following the resolution of her symptoms and the normalization of all laboratory test indicators.

Following a series of diagnostic tests, the patient was confirmed to have SFTS and brucellosis on the tenth day after disease onset and was subsequently discharged on the seventeenth day. Treatment initiated post-diagnosis included rest, doxycycline (100 mg twice daily) and levofloxacin (500 mg once daily) for brucellosis, along with caffeic acid (0.2 g three times daily) to boost white blood cells and platelet counts. Nutritional support was provided through supplements of vitamin C and vitamin B6. No similar cases were identified upon interviewing her family, neighboring villagers, and the hospital staff involved in her care.

In this study of co-infection, we examined patients diagnosed with two distinct diseases at Yidu Central

Hospital of Weifang in 2023. The analysis included 75 cases of brucellosis and 26 cases of SFTS. Both the incidence and distribution of these infectious diseases exhibited temporal and spatial overlap. Brucellosis cases occurred throughout the year, peaking between January and July, whereas SFTS cases were confined to the months of May through October, as shown in Figure 1. Geographically, brucellosis cases were more broadly spread, with the majority (72%) originating from Linqu County and Qingzhou county-level City, Weifang City. In contrast, all reported cases of SFTS were from these same locations.

DISCUSSION

While co-infections involving various zoonotic infectious diseases have been documented (*1*), cases involving simultaneous infections with SFTSV and *Brucella* are yet unreported. To the best of our knowledge, this report describes the first rare instance of a patient co-infected with brucellosis and SFTS. Managing and treating this co-infection proved challenging. Despite the eventual discharge of the patient free of symptoms and laboratory abnormalities, the journey from detection to definitive diagnosis was protracted. This extended diagnostic timeline poses a significant risk to health. It is crucial for the management of both brucellosis and SFTS to focus on early detection, diagnosis, and treatment (*2–3*). Delayed treatment of these conditions can lead to severe outcomes, including chronic infection from *Brucella* and potentially fatal complications from SFTS (*4*). In summary, prompt and accurate diagnosis is essential for effective treatment and recovery.

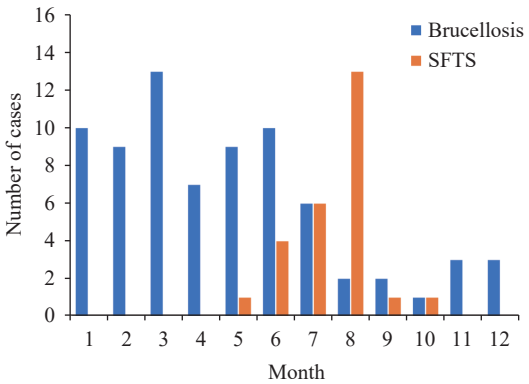

FIGURE 1. Temporal distribution of brucellosis cases and SFTS cases in Yidu Central Hospital of Weifang in 2023. Abbreviation: SFTS=severe fever with thrombocytopenia syndrome.

This case illustrates that brucellosis should be a primary consideration in patients presenting with fever, fatigue, joint pain, and a history of contact with sheep. Conversely, SFTS should be suspected in patients who report tick bites and exhibit thrombocytopenia, tender lymphadenopathy, and elevated levels of alanine aminotransferase, aspartate aminotransferase, lactate dehydrogenase, and creatine kinase. The occurrence of such symptoms suggests the need to evaluate for potential co-infections with multiple pathogens.

Brucellosis and SFTS are neglected zoonotic diseases that have demonstrated a rising incidence in recent years (*5–6*). A spatiotemporal analysis of the occurrence of these diseases among patients at the Yidu Central Hospital of Weifang revealed concurrent spatial and temporal patterns of infection. We hypothesize that an increasing number of similar cases may be identified in the future. Consequently, heightened vigilance is essential to timely detect co-infected patients, thereby preventing misdiagnosis and underdiagnosis. First, healthcare institutions must assume greater responsibility by analyzing disease patterns among local and nearby populations, offering free consultations, and enhancing health education in areas at high risk. These measures will improve awareness and diagnosis of these diseases and ensure the availability of necessary diagnostic reagents. Second, to facilitate early detection, accurate diagnosis, and effective treatment — thereby reducing chronicity and mortality — we recommend the implementation of a joint-examination strategy in regions where both brucellosis and SFTS are prevalent, such as Linqu County and Qingzhou county-level City. Lastly, considering the interconnected nature of human, animal, and environmental health in the transmission of brucellosis and SFTS, it is imperative to adopt a "One Health" approach. This strategy will promote comprehensive health and well-being across these interconnected domains.

In this paper, we present a rare case of co-infection involving brucellosis and SFTS, which contributes to the sparse body of knowledge on the simultaneous presence of multiple zoonotic diseases. This report aims to enhance the recognition and diagnosis of such co-infections among healthcare professionals. The insights gleaned from our study are crucial for the early diagnosis and treatment of these diseases, and they also inform preventive and control strategies. To improve the prevention, control, diagnosis, and treatment of these diseases, we propose several recommendations.

First, it is imperative to conduct public education campaigns for local farmers, emphasizing preventive measures against brucellosis and SFTS. Second, medical practitioners in endemic regions must possess a thorough understanding of local infectious diseases and engage in comprehensive consultations with patients presenting with fever to ensure accurate diagnoses. Third, the development and implementation of rapid and precise methods for detecting multiple pathogens are essential to minimize the risks of misdiagnosis and underdiagnosis.

Conflicts of interest: No conflicts of interest.

Funding: This study was supported by State Key Laboratory of Infectious Disease Prevention and Control (Grant No.33002 to HJ) and Jinan Municipal Health Commission Science and Technology Planning Projects (Grant No.2020-4-113).

doi: 10.46234/ccdcw2024.125

[#] Corresponding author: Hai Jiang, jianghai@icdc.cn.

[1] National Key Laboratory of Intelligent Tracing and Forecasting for Infectious Diseases, National Institute for Communicable Disease Control and Prevention, Chinese Center for Disease Control and Prevention, Beijing, China; [2] Department of Infectious Diseases, Yidu Central Hospital of Weifang, Weifang City, Shandong Province, China; [3] Institute of Bacterial Disease, Jinan Center for Disease Control and Prevention, Jinan City, Shandong Province, China; [4] Tongliao Center for Disease Control and Prevention, Tongliao City, Inner Mongolia Autonomous Region, China.
[&] Joint first authors.

Submitted: January 10, 2024; Accepted: June 11, 2024

REFERENCES

1. Siddiqui A, Randev S, Singla N, Dhavan A, Guglani V, Gupta V. Acute disseminated encephalomyelitis due to a zoonotic co-infection. J Trop Pediatr 2022;69(1):fmad008. https://doi.org/10.1093/tropej/fmad008.
2. Liu Q, He B, Huang SY, Wei F, Zhu XQ. Severe fever with thrombocytopenia syndrome, an emerging tick-borne zoonosis. Lancet Infect Dis 2014;14(8):763 – 72. https://doi.org/10.1016/S1473-3099(14)70718-2.
3. An CH, Shen L, Sun MH, Sun YX, Fan SP, Zhao CX, et al. Exploring risk transfer of human brucellosis in the context of livestock agriculture transition: a case study in Shaanxi, China. Front Public Health 2023;10:1009854. https://doi.org/10.3389/fpubh.2022.1009854.
4. Zhao J, Ge HH, Wang G, Lin L, Yuan Y, Xu YL, et al. Fatal patients with severe fever with thrombocytopenia syndrome in China. Int J Infect Dis 2022;125:10 – 6. https://doi.org/10.1016/j.ijid.2022.10.008.
5. Laine CG, Johnson VE, Scott HM, Arenas-Gamboa AM. Global estimate of human brucellosis incidence. Emerg Infect Dis 2023;29(9):1789 – 97. https://doi.org/10.3201/eid2909.230052.
6. Miao D, Liu MJ, Wang YX, Ren X, Lu QB, Zhao GP, et al. Epidemiology and ecology of severe fever with thrombocytopenia syndrome in China, 2010−2018. Clin Infect Dis 2021;73(11):e3851 – 8. https://doi.org/10.1093/cid/ciaa1561.

Youth Editorial Board

Director Lei Zhou

Vice Directors Jue Liu Tiantian Li Tianmu Chen

Members of Youth Editorial Board

Jingwen Ai	Li Bai	Yuhai Bi	Yunlong Cao
Gong Cheng	Liangliang Cui	Meng Gao	Jie Gong
Yuehua Hu	Jia Huang	Xiang Huo	Xiaolin Jiang
Yu Ju	Min Kang	Huihui Kong	Lingcai Kong
Shengjie Lai	Fangfang Li	Jingxin Li	Huigang Liang
Di Liu	Jun Liu	Li Liu	Yang Liu
Chao Ma	Yang Pan	Zhixing Peng	Menbao Qian
Tian Qin	Shuhui Song	Kun Su	Song Tang
Bin Wang	Jingyuan Wang	Linghang Wang	Qihui Wang
Xiaoli Wang	Xin Wang	Feixue Wei	Yongyue Wei
Zhiqiang Wu	Meng Xiao	Tian Xiao	Wuxiang Xie
Lei Xu	Lin Yang	Canqing Yu	Lin Zeng
Yi Zhang	Yang Zhao	Hong Zhou	

Indexed by Science Citation Index Expanded (SCIE), Social Sciences Citation Index (SSCI), PubMed Central (PMC), Scopus, Chinese Scientific and Technical Papers and Citations, and Chinese Science Citation Database (CSCD)

Copyright © 2024 by Chinese Center for Disease Control and Prevention

All Rights Reserved. No part of the publication may be reproduced, stored in a retrieval system, or transmitted in any form or by any means, electronic, mechanical, photocopying, recording, or otherwise without the prior permission of *CCDC Weekly*. Authors are required to grant *CCDC Weekly* an exclusive license to publish.

All material in *CCDC Weekly* Series is in the public domain and may be used and reprinted without permission; citation to source, however, is appreciated.

References to non-China-CDC sites on the Internet are provided as a service to *CCDC Weekly* readers and do not constitute or imply endorsement of these organizations or their programs by China CDC or National Health Commission of the People's Republic of China. China CDC is not responsible for the content of non-China-CDC sites.

The inauguration of *China CDC Weekly* is in part supported by Project for Enhancing International Impact of China STM Journals Category D (PIIJ2-D-04-(2018)) of China Association for Science and Technology (CAST).

CCDC weekly

Vol. 6 No. 27 Jul. 5, 2024

Responsible Authority
National Disease Control and Prevention Administration

Sponsor
Chinese Center for Disease Control and Prevention

Editing and Publishing
China CDC Weekly Editorial Office
No.155 Changbai Road, Changping District, Beijing, China
Tel: 86-10-63150501, 63150701
Email: weekly@chinacdc.cn

CSSN
ISSN 2096-7071 (Print)
ISSN 2096-3101 (Online)
CN 10-1629/R1